

1 **Carbon dioxide emissions from the flat bottom and shallow**  
2 **Nam Theun 2 Reservoir: drawdown area as a neglected**  
3 **pathway to the atmosphere**

4 **Chandrashekar Deshmukh<sup>1,2,3,a</sup>, Frédéric Guérin<sup>1,4,5</sup>, Axay Vongkhamsao<sup>6</sup>,**  
5 **Sylvie Pighini<sup>6,b</sup>, Phetdala Oudone<sup>6,c</sup>, Saysoulinthone Sopraseuth<sup>6</sup>, Aranud**  
6 **Godon<sup>6,d</sup>, Wanidoporn Rode<sup>6</sup>, Pierre Guédant<sup>6</sup>, Priscia Oliva<sup>1</sup>, Stéphane Audry<sup>1</sup>,**  
7 **Cyril Zouiten<sup>1</sup>, Corinne Galy-Lacaux<sup>2</sup>, Henri Robain<sup>7</sup>, Olivier Ribolzi<sup>1</sup>, Arun**  
8 **Kansal<sup>3</sup>, Vincent Chanudet<sup>8</sup>, Stéphane Descloux<sup>8</sup>, Dominique Serça<sup>2</sup>**

9 [1]{Géosciences Environnement Toulouse (GET), Université de Toulouse (UPS), 14 Avenue  
10 E. Belin, F-31400 Toulouse, France}

11 [2]{Laboratoire d'Aérodynamique - Université de Toulouse - CNRS UMR 5560; 14 Av. Edouard  
12 Belin, F-31400, Toulouse, France}

13 [3]{Centre for Regulatory and Policy Research, TERI University, New Delhi, India}

14 [4]{IRD ; UR 234, GET ; 14 Avenue E. Belin, F-31400, Toulouse, France}

15 [5]{Departamento de Geoquímica, Universidade Federal Fluminense, Niterói-RJ, Brasil}

16 [6]{Nam Theun 2 Power Company Limited (NTPC), Environment & Social Division – Water  
17 Quality and Biodiversity Dept.– Gnommalath Office, PO Box 5862, Vientiane, Lao PDR}

18 [7]{IRD, iEES-Paris, Centre IRD France-Nord, 32 avenue Henri Varagnat, 93143 Bondy  
19 Cedex, France}

20 [8]{Electricité de France, Hydro Engineering Centre, Sustainable Development Dpt, Savoie  
21 Technolac, F-73373 Le Bourget du Lac, France}

22 [a]{now at: Asia Pacific Resources International Limited (APRIL), Indonesia}

23 [b]{now at: Innsbruck University, Institute of Ecology, 15 Sternwartestrasse, A-6020  
24 Innsbruck, Austria and Foundation Edmund Mach, FOXLAB-FEM, Via E. Mach 1, IT-38010  
25 San Michele all'Adige, Italy}

26 [c]{now at: Department of Environmental Science, Faculty of Environmental Sciences,  
27 National University of Laos, Vientiane, Lao PDR}

28 [d]{now at: Arnaud Godon Company, 44 Route de Genas, Nomade Lyon, 69003 Lyon,  
29 France}

30 Correspondence to: F. Guérin (Frederic.guerin@ird.fr)

### 31 **Abstract**

32 Freshwater reservoirs are a significant source of CO<sub>2</sub> to the atmosphere. CO<sub>2</sub> is known to be  
33 emitted at the reservoir surface by diffusion at the air-water interface and downstream of  
34 dams or powerhouses by degassing and along the river course. In this study, we quantified  
35 total CO<sub>2</sub> emissions from the Nam Theun 2 Reservoir (Lao PDR) in the Mekong River  
36 watershed. The study started in May 2009, less than a year after flooding and just a few  
37 months after the maximum level was first reached and lasted until end of 2013. We tested the  
38 hypothesis that soils from the drawdown area would be a significant contributor to the total  
39 CO<sub>2</sub> emissions.

40 Total inorganic carbon, dissolved and particulate organic carbon and CO<sub>2</sub> concentrations were  
41 measured in 4 pristine rivers of the Nam Theun watershed, at 9 stations in the reservoir  
42 (vertical profiles) and at 16 stations downstream of the monomictic reservoir on a weekly to  
43 monthly basis. CO<sub>2</sub> bubbling was estimated during five field campaigns between 2009 and  
44 2011 and on a weekly monitoring, covering water depths ranging from 0.4 to 16m and various  
45 types of flooded ecosystems in 2012 and 2013. Three field campaigns in 2010, 2011 and 2013  
46 were dedicated to the soils description in 21 plots and the quantification of soil CO<sub>2</sub> emissions  
47 from the drawdown area. On this basis, we calculated total CO<sub>2</sub> emissions from the reservoir  
48 and carbon inputs from the tributaries. We confirm the importance of the flooded stock of  
49 organic matter as a source of C fuelling emissions. We show that the drawdown area  
50 contributes, depending on the year, from 40% to 75% of total annual gross emissions in this  
51 flat and shallow reservoir. Since the CO<sub>2</sub> emissions from the drawdown zone are almost  
52 constant throughout the years, the large interannual variations result from the significant  
53 decrease of diffusive fluxes and downstream emissions between 2010 and 2013. This  
54 overlooked pathway in terms of gross emissions would require an in-depth evaluation for the  
55 soil OM and vegetation dynamics to evaluate the actual contribution of this area in terms of  
56 net modification of gas exchange in the footprint of the reservoir, and how it could evolve in  
57 the future.

## 58 **1 Introduction**

59 Carbon dioxide (CO<sub>2</sub>) emissions from inland waters were recently revisited and it appears that  
60 emissions from freshwater reservoirs contribute significantly despite the disproportionately  
61 small surface area of these systems (Barros et al., 2011; Raymond et al., 2013; Deemer et al.,  
62 2016). The CO<sub>2</sub> production and subsequent emissions in reservoirs result from the  
63 degradation of the flooded organic matter (OM) and the OM originating from the watershed  
64 (Galy-Lacaux et al., 1997b; Abril et al., 2005; Guérin et al., 2008; Barros et al., 2011; Teodoru  
65 et al., 2011). As the amount of labile OM originating from the flooded soils and biomass  
66 decreases with time due to the progressive mineralisation of the carbon stock, emissions  
67 decrease progressively with reservoirs ageing (Abril et al., 2005; Barros et al., 2011). CO<sub>2</sub>  
68 emissions are higher in tropical reservoirs than in temperate and boreal ones, a latitudinal  
69 difference attributed to the enhancement of OM degradation with temperature (Barros et al.,  
70 2011; Marotta et al., 2014; Yvon-Durocher et al., 2014). Emissions occur through diffusion at  
71 the air-water interface of the reservoir and from rivers downstream of dams (Abril et al.,  
72 2005; Guérin et al., 2006; Kemenes et al., 2011). At the surface of reservoirs, it is well known  
73 that emissions vary significantly spatially and temporally. Spatial variations can be higher  
74 than temporal variations (Roland et al., 2010; Teodoru et al., 2011; Zhao et al., 2013; Pacheco  
75 et al., 2015). Thus, the integration of both temporal and spatial variations is mandatory for the  
76 determination of accurate emission factors.

77 In some reservoirs with large water level variations, large surface areas of soils known as  
78 drawdown zones are periodically exposed to the atmosphere (for example, Three- Gorges and  
79 Nam Theun 2 reservoirs). Recently, the importance of the drawdown emissions was pointed  
80 out as a significant source of CH<sub>4</sub> in the Three Gorges Dam in China (Chen et al., 2009; Chen  
81 et al., 2011; Yang et al., 2012) and a very minor source at Nam Theun 2 Reservoir (NT2R)  
82 (Serça et al., 2016). CO<sub>2</sub> emission from the drawdown area was only measured in agricultural  
83 plots of the drawdown area of the Three Gorges Dam (Li et al., 2016). However, the  
84 hypothesis of significant CO<sub>2</sub> emissions from those soils seasonally flooded and exposed to  
85 air was never tested in unmanaged drawdown area representative of tropical reservoirs with  
86 large water level variations. In the present study, we measured CO<sub>2</sub>, organic and inorganic  
87 carbon concentrations and physico-chemical parameters at 9 stations in the NT2R and 16  
88 stations downstream of the dam and the powerhouse. This weekly to fortnightly sampling was  
89 conducted in order to estimate emissions from the reservoir surface and downstream

90 emissions during 4.5 years of monitoring after impoundment. We also measured CO<sub>2</sub>  
91 emissions from the large drawdown area of the NT2R that represented seasonally up to 65%  
92 of the maximum reservoir area during the study. The spatial, seasonal and interannual  
93 variation of emissions by all the above-listed pathways and their contribution to total gross  
94 CO<sub>2</sub> emissions will be discussed.

## 95 **2 Material and Methods**

### 96 **2.1 Study site**

97 The NT2R is located in Lao People's Democratic Republic (Lao PDR), it was impounded in  
98 April 2008 and was commissioned in April 2010. It floods 489 km<sup>2</sup> of very diverse types of  
99 ecosystems including forest, agricultural soils and wetlands (Descloux et al., 2011).  
100 Geological formations responsible for the soil development in the NT2R area are mainly  
101 composed by more or less consolidated sedimentary rocks (Lovatt Smith et al., 1996; Smith  
102 and Stokes, 1997). The parental rocks belong to the Khorat group and Phon Hong group  
103 formations (Cretaceous) with two main lithologies: (1) late cretaceous Maha Sarakham  
104 formation (i.e., evaporites and mudstones) and (2) aptian Khot Kruat formation (i.e., mainly  
105 fluvial formation of red siltstones and sandstones)

106 The NT2R, described in detail in Descloux et al. (2016); Deshmukh et al. (2016); Guérin et al.  
107 (2016) is under the influence of a monsoon subtropical climate with three main seasons: the  
108 cold dry season (CD, from mid-Oct. to mid-Feb.), the warm dry season (WD, from mid-Feb.  
109 to mid-June) and the warm wet season (WW, from mid-June to mid-Oct.). Owing to the large  
110 seasonal variations of the river discharges in the region, the reservoir area ranged seasonally  
111 between 489 in the WW season to 170 km<sup>2</sup> in the WD season during the course of the study.  
112 On the opposite, the surface of the drawdown area reached its maximum (320 km<sup>2</sup>) when the  
113 water level was the lowest. During the monitoring, the wettest years were 2011 and 2013 with  
114 an average water discharge in the reservoir of ~270 m<sup>3</sup> s<sup>-1</sup> whereas the driest year was 2012  
115 with a discharge 230 m<sup>3</sup> s<sup>-1</sup>. In 2011, in this single year the reservoir had the largest water  
116 level variations with the largest surface area of the monitoring in the wet season (491 km<sup>2</sup>)  
117 and the smallest of the monitoring in the WD season (168 km<sup>2</sup>). The NT2R is a trans-basin  
118 reservoir with two downstream sections: one below the powerhouse and one below the Nakai  
119 Dam (Figure 1). Except during the occasional use of the spillways, only 2m<sup>3</sup> s<sup>-1</sup> of water are  
120 discharged downstream of the Nakai Dam in the Nam Theun River and around 240 m<sup>3</sup> s<sup>-1</sup> are

121 released to the powerhouse, the regulating pond and finally the artificial downstream channel  
122 before water reaches the Xe Bangfai River (Figure 1).

## 123 **2.2 Sampling strategy**

124 The CO<sub>2</sub> and O<sub>2</sub> concentrations in water and the water temperature were determined in  
125 surface waters of six pristine rivers and three rivers under the influence of the reservoir (10  
126 stations) and in the artificial channel (5 stations) whereas it was done along vertical profiles in  
127 the reservoir (9 stations) and the regulation pond (1 station) (Figure 1). At all sites located  
128 downstream of the powerhouse, sampling was done weekly (from March 2010 to December  
129 2013) whereas it was done fortnightly in incoming pristine rivers and in the reservoir (from  
130 May 2009 to December 2013). The stations RES1-RES3 flooded dense forest, the stations  
131 RES4-RES6 flooded degraded forest, the station RES7 flood swamps and the station RES8  
132 flooded a rice field area (Descloux et al., 2011;Guérin et al., 2016). The station RES9 is  
133 located at the water intake, an area of continuous vertical mixing of the water column, where  
134 CH<sub>4</sub> emissions are enhanced (Guérin et al., 2016). Degassing of CO<sub>2</sub> was calculated below  
135 the Nakai Dam, just below the turbines at TRC1, below the regulating dam (RD on Figure 1)  
136 and at the aeration weir (AW on Figure 1). Bubbling of CO<sub>2</sub> was determined during five field  
137 campaigns covering different seasons and sites in 2009, 2010 and 2011, and during a weekly  
138 monitoring from March 2012 to August 2013 at seven stations. In the drawdown area, soil  
139 description was conducted in June 2010 at six sites and CO<sub>2</sub> emissions were repeatedly  
140 measured at 21 plots over those sites in June 2010, 2011 and 2013.

## 141 **2.3 In situ measurements and water analysis**

142 Vertical profiles of O<sub>2</sub>, pH and temperature were measured in situ at all sampling stations  
143 with a multi-parameter probe Quanta® (Hydrolab, Austin, Texas) since January 2009. In the  
144 reservoir, the vertical resolution was 0.5 m down to 5 m and and 1 m deeper. Surface and  
145 deep-water samples for CO<sub>2</sub>, dissolved organic carbon (DOC), particulate organic carbon  
146 (POC) and dissolved inorganic carbon (DIC) concentrations were taken with a surface water  
147 sampler (Abril et al., 2007) and a UWITEC™ sampling bottle, respectively. Water samples  
148 for CO<sub>2</sub> determination were stored in serum glass vials, capped with butyl stoppers, sealed  
149 with aluminium crimps and preserved (Guérin and Abril, 2007). CO<sub>2</sub> concentrations were  
150 determined by the headspace technique and using the solubility coefficient of Weiss (1974) as  
151 in Guérin et al. (2006). The CO<sub>2</sub> partial pressure in headspace was determined by gas

152 chromatography (GC) (SRI 8610C gas chromatograph, Torrance, CA, USA) equipped with a  
153 flame ionization detector and a methanizer (Chanudet et al., 2011). Commercial gas standards  
154 (400, 1000 and 3000 ppmv, Air Liquid "crystal" standards) were injected after every 10  
155 samples for calibration. Detection limit was  $< 1$  ppmv in headspace and duplicate injection of  
156 samples showed reproducibility better than 5%. For TIC, DOC and POC, analyses were  
157 performed with a Shimadzu TOC-V<sub>CSH</sub> analyser. Filtered (0.45  $\mu\text{m}$ , Nylon) and unfiltered  
158 samples were analysed for TIC and TOC. POC was calculated by the difference between  
159 TOC and DOC concentrations in unfiltered and filtered samples. The detection limit was 8  
160  $\mu\text{mol L}^{-1}$  and uncertainty was 2.0  $\mu\text{mol L}^{-1}$  on TOC and DOC and 2.8  $\mu\text{mol L}^{-1}$  on POC.

## 161 **2.4 Organic and inorganic carbon inputs from the watershed to the reservoir**

162 Carbon inputs were calculated on a monthly basis using monthly average of the river  
163 discharge of the four main tributaries of the NT2R. The Nam Theun River contributed 32%  
164 (27  $\text{m}^3 \text{s}^{-1}$ ) of the total discharge while Nam Xot (22  $\text{m}^3 \text{s}^{-1}$ ), Nam On (19  $\text{m}^3 \text{s}^{-1}$ ) and Nam  
165 Noy (25  $\text{m}^3 \text{s}^{-1}$ ) not monitored for biogeochemistry) contributed 23%, 22 and 24%  
166 respectively. For the Nam On River, the specific water discharge and POC, DOC, TIC and  
167  $\text{CO}_2$  from this river were used. For the other rivers, the specific water discharge of each river  
168 was used together with the average DOC, POC, TIC and  $\text{CO}_2$  from Nam Theun, Nam Phao  
169 and Nam Xot Rivers all located in the Nam Theun watershed. Note that the Nam Phao  
170 reaches the Nam Theun River downstream of the Nakai Dam but we used this dataset together  
171 with the ones from other rivers to calculate the carbon inputs since the physico-chemical  
172 parameters and carbon concentrations are not different from other rivers in the watershed.

## 173 **2.5 Diffusive fluxes and degassing**

174 Diffusive fluxes at the air-water interface of the reservoir were calculated from the surface  
175  $\text{CO}_2$  concentrations, wind speed and rainfall rates using the gas transfer velocity formulations  
176 of Guérin et al. (2007) and MacIntyre et al. (2010) as already described for  $\text{CH}_4$  fluxes from  
177 this reservoir (Deshmukh et al., 2014; Guérin et al., 2016). Based on physical modelling and in  
178 situ measurements (Chanudet et al., 2012), we determined that the station RES9 located at the  
179 water intake is representative of an area of about 3  $\text{km}^2$  (i.e. 0.6 % of the reservoir water  
180 surface at full reservoir water level), whatever the season (Guérin et al., 2016). This area was  
181 therefore used to extrapolate specific diffusive fluxes from this station. For other stations,  
182 diffusive fluxes are calculated with the daily meteorological parameters and reservoir water

183 surface area from the capacity curve. Degassing downstream of the powerhouse, the  
184 regulating dam and the aeration weir, all located along the artificial channel and downstream  
185 of the Nakai Dam (Figure 1), were computed using the CO<sub>2</sub> concentration upstream and  
186 downstream of these civil structures and the water discharge as in Deshmukh et al. (2016) for  
187 CH<sub>4</sub>. The diffusion from the rivers and artificial channel below the powerhouse and the dam  
188 was calculated using a constant gas transfer velocity of 10 cm h<sup>-1</sup> (Deshmukh et al., 2016).

## 189 **2.6 CO<sub>2</sub> bubbling**

190 Bubbling of CO<sub>2</sub> was determined with funnels (Deshmukh et al., 2014) during five field  
191 campaigns covering different seasons (between May 2009 and June 2011), and during a  
192 weekly monitoring from March 2012 to August 2013. During this monitoring, spatial  
193 variation was explored through measurements spread over six stations (Fig. 1) representative  
194 of the different types of flooded ecosystems (dense and medium forests, light and degraded  
195 forest and agricultural lands as determined by Descloux et al. (2011)), and with different  
196 depths (from 0.4 to 16 m) at each station. We stopped measuring bubbling at sites deeper than  
197 16m after no ebullition was observed during the first three campaigns. Bubble samples were  
198 taken with a 50 mL-syringe and the syringe was immediately connected to a N<sub>2</sub>-preflushed  
199 10-mL serum vial, leading to a dilution factor of 5/6 (Guérin et al., 2007). Gas samples were  
200 analysed with the GC described above.

## 201 **2.7 Soil descriptions and CO<sub>2</sub> fluxes from the drawdown area**

202 Since the drawdown area of the NT2R could represent up to 65% of the surface area of the  
203 reservoir at the end of the WD season, emissions from this major area under the influence of  
204 flooding were evaluated. Soil types were determined together with CO<sub>2</sub> emissions. Soil  
205 description was carried out in June 2010 at 6 sites and soils from the station RES4S plot were  
206 characterized in detail in June 2013 (Figure 1, Table 1). Four sites were selected in the Nam  
207 Theun River riparian's area (NMR, RES2S, RES4S, RES8S'), one site in the flooded primary  
208 forest (RES3S) and one site in the flooded agricultural area (RES8S). Soil study was  
209 conducted through soil catenae of 2 to 4 soils profiles from the pristine soils on top ("upland"  
210 samples) to the shoreline of the reservoir ("shoreline" samples). One or two other soils  
211 profiles were performed in between ("interm.up" and "interm.down" samples, with interm  
212 standing for intermediate). Soil sampling was performed with an Edelman soil corer down to  
213 a depth of 1m, but only 0-20cm depth samples were considered in this study. Information on

214 horizon depth, soil texture and structure (e.g., compactness, porosity), color (Munsell chart  
215 for soil color), soil fauna activity and pedological features (e.g., redoximorphic features,  
216 concretions) were provided through soil description in the field. Samples for C, N, and pH  
217 were selected following the horizons apparition for each soil profile. They were manually  
218 decompacted and stored in plastic bags. Back in the laboratory, soil samples were dried out at  
219 room temperature under a laminar flow hood, sieved at 2 mm and properly split in two  
220 representative subsamples. One of the subsamples was crushed with an agate mortar before  
221 chemical analysis. The non-crushed subsample was dedicated to soil pH and granulometric  
222 measurements. C and N analysis where performed with a Elementar Vario EL III C/N/S  
223 analyser and soil pH measurements were performed in ultrapure water (18.2 MΩ) following  
224 ISO 11464 standard procedure.

225 At the 6 sites, fluxes were measured along the soil moisture gradient between the shoreline  
226 and the zone not impacted by the reservoir water level fluctuation. Three to four sites with  
227 contrasting moisture content were selected at each site. At those six sites, fluxes were  
228 measured at 21 plots in total and 40 CO<sub>2</sub> fluxes were gathered, mostly in duplicates (from 1 to  
229 4 replicates) (Table 2). CO<sub>2</sub> emissions were measured during 3 field campaigns in 2010, 2011  
230 and 2013 using stainless steel chamber (volume 12 L, 0.08 m<sup>2</sup>) described in Serça et al.  
231 (1994) and Serça et al. (2016). At each site, two chambers were deployed in parallel and the  
232 collars were installed at least 1 hour prior to measurement. Air samples were taken and stored  
233 with the same methodology as for bubbling samples every 15 minutes in each chamber before  
234 subsequent GC analysis. It has to be noted that soil studies and measurement of fluxes were  
235 restricted for safety reason due to the high density of unexploded ordnances (UXO) from the  
236 sixties and seventies in that area.

### 237 **3 Results**

#### 238 **3.1 Temperature, oxygen, pH, organic and inorganic carbon in the Nam Theun** 239 **watershed and carbon inputs to the reservoir**

240 In the rivers of the Nam Theun watershed, the water temperature was 24.5±0.2°C ranging  
241 from 13.5 to 32.0°C and pH was 6.83±0.03 (4.75-8.95, n=405). The Nam On River was, on  
242 average, less oxygenated (77±2%) than the others. It is characterized by the highest DOC  
243 concentrations (222±11 μmol L<sup>-1</sup>, n=93), and amongst the highest CO<sub>2</sub> concentrations (59±6  
244 μmol L<sup>-1</sup>, n=107) and the lowest TIC concentration (237±11 μmol L<sup>-1</sup>, n=107) (Figure 2). The



245 Nam Phao and the Nam Theun Rivers are not significantly different in terms of POC, DOC,  
246 TIC and CO<sub>2</sub> concentrations (Figure 2). During the monitoring, the average DOC in the Nam  
247 Phao was 87±4 μmol L<sup>-1</sup> (n=82) and 108±4 μmol L<sup>-1</sup> (n=97) in the Nam Theun, that is more  
248 than two times lower than in the Nam On. TIC was 40% higher in the Nam Theun and Nam  
249 Phao Rivers than in the Nam On (Nam Phao: 380±12 μmol L<sup>-1</sup>, n=82; Nam Theun: 379±15  
250 μmol L<sup>-1</sup>, n=97) (Figure 2). CO<sub>2</sub> in the Nam Theun River (54±5 μmol L<sup>-1</sup>, n=105) and in the  
251 Nam Phao (46±5 μmol L<sup>-1</sup>, n=86) contributed around 15% of TIC whereas it was almost 25%  
252 in the Nam On. The Nam Xot River had amongst the lowest DOC (90±3 μmol L<sup>-1</sup>, n=93),  
253 TIC (272±12 μmol L<sup>-1</sup>, n=94) and CO<sub>2</sub> (45±3 μmol L<sup>-1</sup>, n=110) concentrations (Figure 2).  
254 Comparing results from all rivers, we could not find any significant differences in POC  
255 concentration. In all rivers during this monitoring, the average POC was 28±2 μmol L<sup>-1</sup>  
256 (n=200) and contributed less than 20% of the total organic carbon (DOC+POC) in this  
257 watershed (Figure 2). We could not identify any clear seasonal pattern for POC, DOC TIC  
258 and CO<sub>2</sub> concentrations in the four rivers of the Nam Theun watershed (Figure 2).

259 As reported in Descloux et al. (2016), the average total water discharge in the reservoir is 238  
260 m<sup>3</sup> s<sup>-1</sup> ranging from 6 m<sup>3</sup> s<sup>-1</sup> during the WD seasons to 2061 m<sup>3</sup> s<sup>-1</sup> during the WW seasons.  
261 Carbon input to the reservoir as DOC, POC and TIC ranged from 32.2±1.3 GgC yr<sup>-1</sup> in 2010  
262 to 46.2±1.5 GgC yr<sup>-1</sup> in the wet year 2011 (Figure 3). During the monitoring, TIC represented  
263 60 to 70% of the carbon inputs to the reservoir (Figure 3).

### 264 **3.2 Vertical profiles of temperature, O<sub>2</sub>, pH, CO<sub>2</sub> and organic carbon in the** 265 **reservoir water column**

266 At the stations RES1-RES8, the typical vertical distributions of temperature, O<sub>2</sub>, DOC, POC  
267 and CO<sub>2</sub> for the three seasons at various sampling stations are shown in Figure 4. As already  
268 described in detail in Guérin et al. (2016), during the four years of monitoring, the reservoir  
269 water column was thermally stratified during the warm seasons with thermocline at 4.5±2.6  
270 and 5.8±4.8 m depths during the WD and WW seasons, respectively. As a consequence of  
271 thermal stratification, the warm epilimnic waters are well oxygenated (>80% saturation)  
272 whereas the hypolimnion is anoxic (Figure 4). Occasionally, sporadic and local  
273 destratification occurred during high water inflow in the WW season. During the CD season,  
274 temperature and O<sub>2</sub> decreased gradually with depth or O<sub>2</sub> concentration was constant from the  
275 surface to the bottom of the water column (Figure 4). After the power plant commissioning,

276 the water column located near the Turbine Intake (RES9) got totally mixed as revealed by the  
277 homogeneous temperature and O<sub>2</sub> profiles from the surface to the bottom (Figure 4). pH  
278 always decreased from the surface to the bottom with, on average during the monitoring,  
279 surface pH = 6.66±0.02 (5.21-8.76, n=1316) and hypolimnic pH = 6.15±0.01 (4.88-8.00,  
280 n=1488).

281 Over the monitoring period at the stations RES1-RES8, the average CO<sub>2</sub> concentration in the  
282 water column was 389±9 μmol L<sup>-1</sup> and ranged from 0.3 to 4770 μmol L<sup>-1</sup> (n=3698). It  
283 decreased from 544±24 μmol L<sup>-1</sup> in 2010 to 154±9 μmol L<sup>-1</sup> in 2013. During the WD and  
284 WW seasons, CO<sub>2</sub> concentrations increased with water depth and often showed a maximum  
285 gradient at or just below the thermocline (Figure 4). For the years 2010 to 2013, the average  
286 CO<sub>2</sub> concentrations in the water column during the WD and WW seasons were always 50%  
287 higher than in the CD season (Figure 4). DOC concentrations averaged 181±1 μmol L<sup>-1</sup> and  
288 ranged from 12.5 to 569 μmol L<sup>-1</sup> (n=3068). For the years 2010, 2011 and 2012 we observed  
289 a significant decrease of DOC in the water column from year to year with average DOC  
290 concentrations 208±3 μmol L<sup>-1</sup> in 2010, 190±3 μmol L<sup>-1</sup> in 2011 and 177±2 μmol L<sup>-1</sup> in 2012.  
291 In 2013, the DOC was not significantly lower than in 2012 (175±2 μmol L<sup>-1</sup>). From 2010 to  
292 2013, DOC concentrations were about 25% higher in the WD and WW seasons than in the  
293 CD season. Whatever the year, the average epilimnic DOC concentration was 30% higher  
294 than in hypolimnic water. POC concentration was 63±2 μmol L<sup>-1</sup> (n = 2488). POC in  
295 hypolimnic waters (92±3 μmol L<sup>-1</sup>) was almost twice higher than in the epilimnion (45±2  
296 μmol L<sup>-1</sup>) (p < 0.0001, t-test). The POC in the epilimnion decreased significantly from 41±4  
297 μmol L<sup>-1</sup> in 2010 to 23±2 μmol L<sup>-1</sup> in 2013 in the epilimnion (p < 0.0001). POC in  
298 hypolimnic waters did not show any consistent trend with yearly average values being 87±6  
299 μmol L<sup>-1</sup> in 2010, 67±6 μmol L<sup>-1</sup> in 2011, 104±7 μmol L<sup>-1</sup> in the wet year 2012 and 83±5  
300 μmol L<sup>-1</sup> in 2013. No clear seasonal variation was observed.

301 At the station RES9 where the presence of the water intake enhances vertical mixing of the  
302 water column leading to the transport of bottom water to the surface, the water column is not  
303 thermally stratified and always oxygenated from the surface to the bottom after the reservoir  
304 was commissioned in April 2010 (Guérin et al., 2016) (Figure 4). Since commissioning, O<sub>2</sub>  
305 saturation was 60±2 % over the water column. The water column was significantly more  
306 oxygenated during the overturn in the CD (74±3%) than in the WW and WD season (56±2%)

307 ( $p < 0.0001$ , t-test) and significantly more oxygenated ( $p < 0.0001$ ) in the wet year 2011  
308 ( $70 \pm 3\%$  on average) than in 2010 and 2012 ( $56 \pm 3\%$  on average). In 2013, which was an  
309 average hydrological year, the water column was well oxygenated with  $71 \pm 1\%$  suggesting of  
310 improvement of the water quality.  $\text{CO}_2$  concentrations were almost constant from the surface  
311 to the bottom and averaged  $216 \pm 13 \mu\text{mol L}^{-1}$  over the whole monitoring period ( $n = 512$ )  
312 (Fig. 4).  $\text{CO}_2$  concentration in the water column decreased from  $311 \pm 32 \mu\text{mol L}^{-1}$  in 2010  
313 down to  $28 \pm 2 \mu\text{mol L}^{-1}$  in 2013. Concentrations in the WW and WD seasons were similar  
314  $204 \pm 14 \mu\text{mol L}^{-1}$  and more than two times higher than during the CD season ( $105 \pm 6 \mu\text{mol L}^{-1}$ ).  
315 POC concentration was  $25 \pm 1 \mu\text{mol L}^{-1}$  ( $n=431$ ) and DOC was  $157 \pm 2 \mu\text{mol L}^{-1}$  ( $n=642$ )  
316 over the whole water column and both follow the same seasonal variations and temporal  
317 variations as described for the other stations.

### 318 **3.3 Reservoir surface $\text{CO}_2$ concentration and diffusive fluxes**

319 The reservoir surface  $\text{CO}_2$  concentrations ( $n=1067$ ) ranged from 0.3 to  $970 \mu\text{mol L}^{-1}$  (Figure  
320 5a,b) and diffusive fluxes ranged from  $-40.4$  up to  $2694.9 \text{ mmol m}^{-2} \text{ d}^{-1}$  (Figure 5c,d). Most of  
321 the dataset (85% of all measurements) showed  $\text{CO}_2$  supersaturation with respect to the  
322 atmosphere. In 2009 (from May to December), surface concentrations and diffusive fluxes  
323 from all nine sampling stations located in the reservoir were statistically similar ( $p > 0.05$ ,  
324 ANOVA test). The average surface concentration was  $68.2 \pm 47.9 \mu\text{mol L}^{-1}$  and the diffusive  
325 flux was  $101.6 \pm 137.7 \text{ mmol m}^{-2} \text{ d}^{-1}$ .

326 From 2010 to 2013 at the stations RES1 to RES8, the yearly average surface  $\text{CO}_2$   
327 concentrations decreased significantly from  $62.7 \pm 3.6$  to  $32.7 \pm 3.2 \mu\text{mol L}^{-1}$  while diffusive  
328 fluxes decreased from  $89.8 \pm 10$  to  $13.7 \pm 4.7 \text{ mmol m}^{-2} \text{ d}^{-1}$  without any significant spatial  
329 variations ( $p > 0.05$ , ANOVA test). Over the 2010-2012 period, the highest concentration and  
330 fluxes were always observed in the WD season ( $70 \pm 3 \mu\text{mol L}^{-1}$  and  $90 \pm 9 \text{ mmol m}^{-2} \text{ d}^{-1}$ ), they  
331 decreased down to  $51 \pm 3 \mu\text{mol L}^{-1}$  and  $65 \pm 8 \text{ mmol m}^{-2} \text{ d}^{-1}$  in the WW and reached their  
332 minima in the CD season ( $45 \pm 3 \mu\text{mol L}^{-1}$  and  $22 \pm 2 \text{ mmol m}^{-2} \text{ d}^{-1}$ ) (Figure 5 a,c). In 2013, the  
333 reservoir was a net  $\text{CO}_2$  sink from March to August ( $-11 \pm 2 \text{ mmol m}^{-2} \text{ d}^{-1}$ ,  $n=96$ ) and  
334 emissions in the CD season was  $66 \pm 9 \text{ mmol m}^{-2} \text{ d}^{-1}$  ( $n=41$ ) that is three times higher than  
335 usually observed for that season.

336 At the water intake (RES9) after the commissioning, surface concentrations and diffusive  
337 fluxes were statistically different from the other stations and were significantly higher as

338 already observed for CH<sub>4</sub> (Guérin et al., 2016). The average surface CO<sub>2</sub> concentrations at  
339 RES9 were 287±350 and 184±234 μmol L<sup>-1</sup> for the year 2010 and 2011, respectively that is  
340 three-five fold higher than the average at the other stations (Figure 5b). In 2012, surface CO<sub>2</sub>  
341 concentrations at RES9 dropped down to 65±23 μmol L<sup>-1</sup>, still almost twice the concentration  
342 at the other stations. In 2013, surface concentration at RES9 was not statistically different  
343 than at the other station in the reservoir (33±4 μmol L<sup>-1</sup> in 2013). On an annual basis, the  
344 diffusive fluxes at RES9 decreased from an average of 745±195 to 18±9 mmol m<sup>-2</sup> d<sup>-1</sup>  
345 between 2010 and 2013 (Figure 5d). The same seasonality as described before was observed  
346 at RES9 with an exacerbated effect at the transition between the WD and WW seasons since  
347 diffusive fluxes were then up to 17-fold higher than the average fluxes at the other stations for  
348 that same period (Figure 5c,d).

349 Monthly emissions by diffusive fluxes varied by two orders of magnitude between 2009 and  
350 2012. Superimposed on the general decrease of emissions with time, we observed very  
351 significant seasonal variations with emissions peaking during the transition between the WD  
352 and WW seasons, even though the reservoir water surface was at its minimum (Figure 5e).  
353 The annual diffusive CO<sub>2</sub> emission from the reservoir was 730.0±46.2 Gg(CO<sub>2</sub>) year<sup>-1</sup> in 2009  
354 and dropped down by a factor of six in 2013 (118±11.5 Gg(CO<sub>2</sub>) year<sup>-1</sup>) (Figure 5f).

### 355 **3.4 O<sub>2</sub>, pH, organic carbon and CO<sub>2</sub> downstream of the reservoir**

356 After the commissioning, immediately downstream of the power station (station TRC1), the  
357 average O<sub>2</sub> concentration was 174±58 μmol L<sup>-1</sup>, that is, 67±20% saturation (n=189) and pH  
358 was 6.55±0.04 (n=234). Further downstream, the O<sub>2</sub> concentration always increased and the  
359 O<sub>2</sub> saturation downstream of station DCH4 located 30 km from the turbines was always  
360 around 100% saturation in the artificial downstream channel (average 100.4%, n=146). Just  
361 below the regulating dam, in the Nam Kathang River (NKT3), the average O<sub>2</sub> concentration  
362 was 237 μmol L<sup>-1</sup>, that is, 93% saturation (n=120). There was no marked interannual change  
363 in the O<sub>2</sub> concentration. At DCH4, pH increased to 7.17±0.04 (n=186).

364 On average at all the stations in between TRC1 and DCH4, DOC concentration was 159±2  
365 μmol L<sup>-1</sup> (n=1366) over all stations for all years between 2009 and 2013. DOC decreased  
366 from 187±2 μmol L<sup>-1</sup> in 2010 (n=272) to 157±2 μmol L<sup>-1</sup> in 2013 (n=303). Average POC was  
367 25±1 μmol L<sup>-1</sup> (n=818) for all years between 2009 and 2013, and followed interannual

368 variations already observed for the reservoir, i.e. higher POC concentration in the WW season  
369 of 2012.

370 CO<sub>2</sub> concentration below the Powerhouse (TRC1), which receives water from the station  
371 RES9 in the reservoir after the water transiting through the turbines, varied by almost three  
372 orders of magnitude; ranging from 1.4 to 856 μmol L<sup>-1</sup> with an average of 153±14 μmol L<sup>-1</sup> (n  
373 =199). The CO<sub>2</sub> concentrations varied seasonally with maximum concentrations at the end of  
374 the WD season, and minimum at the end of the CD season. Below the powerhouse, along the  
375 longitudinal transects from TRC1 to DCH4, surface CO<sub>2</sub> concentration decreased by a factor  
376 of three within a distance of 30 km during the WD and WW seasons (from 267±34 to 90±10  
377 μmol L<sup>-1</sup> and from 235±28 to 70±8 μmol L<sup>-1</sup> respectively for WD and WW). In the CD  
378 season when CO<sub>2</sub> concentrations were lower, the decrease in concentration with distance from  
379 the dam was only by a factor of two (from 49±8 to 30±4 μmol L<sup>-1</sup>). Between 2010 and 2013  
380 for all stations in the downstream channel (TRC1 to DCH4), annual average CO<sub>2</sub>  
381 concentrations decreased by a factor of 7 from 182±9 μmol L<sup>-1</sup> to 24±2 μmol L<sup>-1</sup>. On average,  
382 CO<sub>2</sub> concentration reached down to 56±5 μmol L<sup>-1</sup> at DCH4 which is in the same order of  
383 magnitude as the concentrations found in the pristine Xe Bangfai River (XBF1, 60±2 μmol L<sup>-1</sup>  
384 <sup>1</sup>, n=64), Nam Kathang Noy River (NKT1, 35±3 μmol L<sup>-1</sup>, n=47) and Nam Kathang Gnai  
385 River (NKT2, 82±10 μmol L<sup>-1</sup>, n=70).

386 Immediately downstream of the Nakai Dam (NTH3) after the commissioning, the average O<sub>2</sub>  
387 concentration was 224 μmol L<sup>-1</sup>, that is 87% saturation (n=73), and the concentration  
388 increased further downstream. pH was 6.84±0.06 (n=166). Average DOC concentration was  
389 166±2 μmol L<sup>-1</sup> (n=653) and decreased from 197±4 μmol L<sup>-1</sup> in 2010 (n=147) to 162±3 μmol  
390 L<sup>-1</sup> (n=127) in 2013. The average POC concentration was 50±5 μmol L<sup>-1</sup> (n=7) and CO<sub>2</sub>  
391 concentration was 67±9 μmol L<sup>-1</sup> (n=77). The CO<sub>2</sub> concentration decreased by a factor of two  
392 (40±5 μmol L<sup>-1</sup>, n=54) within the next 10 km below the dam (down to NTH4, Figure 1) where  
393 pH was 7.19±0.06 (n=97). At NTH4, the observed concentrations were in the same order of  
394 magnitude than the concentrations in the pristine rivers in the same watershed (53±6 μmol L<sup>-1</sup>  
395 at NPH1 in the Nam Phao River, n=59).

### 396 3.5 CO<sub>2</sub> emissions downstream of the reservoir

397 After the commissioning, the annual average diffusive fluxes downstream of the powerhouse  
398 decreased from  $482 \pm 603 \text{ mmol m}^{-2} \text{ d}^{-1}$  in the year 2010 ( $-32$ – $33762 \text{ mmol m}^{-2} \text{ d}^{-1}$ ) to  $32 \pm 8$   
399  $\text{mmol m}^{-2} \text{ d}^{-1}$  ( $-39$ – $216 \text{ mmol m}^{-2} \text{ d}^{-1}$ ) in 2013 (not show). They followed the same seasonal  
400 dynamics as the CO<sub>2</sub> concentrations and they decrease with the distance from the  
401 powerhouse. Total emissions by diffusion from the downstream channel decreased from  
402  $14 \pm 12 \text{ Gg(CO}_2\text{) year}^{-1}$  in 2010 to  $1.3 \pm 0.5 \text{ Gg(CO}_2\text{) year}^{-1}$  in 2013 (Figure 6a). Degassing in  
403 the whole downstream channel (including degassing below the turbines, the regulating pond  
404 and the aeration weir) reached up to  $28.5 \text{ Gg(CO}_2\text{) month}^{-1}$  just after the commissioning of the  
405 reservoir when the water was released for the first time (Figure 6a). During the monitoring,  
406 60-90% of the annual degassing occurred within 3-4 months of transition between the WD  
407 and WW seasons corresponding to the seasons when the hypolimnic waters were the most  
408 enriched in CO<sub>2</sub> (Figure 6a). Total degassing decreased from  $80 \pm 36 \text{ Gg(CO}_2\text{) year}^{-1}$  in 2010  
409 to  $8 \pm 4 \text{ Gg(CO}_2\text{) year}^{-1}$  in 2013 (Figure 6b).

410 Disregarding periods of spillway releases from April to June 2009 for water level regulation  
411 and in September-October 2011 during the flood, degassing downstream of the Nakai Dam  
412 (up to  $0.48 \text{ Gg(CO}_2\text{) month}^{-1}$ ) is usually 10 times lower than degassing in the downstream  
413 channel because of (1) the low continuous water discharge at the Nakai Dam ( $2 \text{ m}^3 \text{ s}^{-1}$ ) and  
414 (2) the withdrawal of the water from the reservoir epilimnion (Deshmukh et al., 2016) (Figure  
415 6a). However, during the use of spillways for water level regulation in the reservoir,  
416 degassing reached up to  $26 \text{ Gg(CO}_2\text{) month}^{-1}$  in 2009 before the commissioning and 4 to 10  
417  $\text{Gg(CO}_2\text{) month}^{-1}$  during the occasional uses in October 2010 and September 2011 (Figure  
418 6a). As determined from the longitudinal profiles of CO<sub>2</sub> concentrations downstream of the  
419 dam, diffusive emissions from the Nam Theun River that are actually attributable to the  
420 NT2R occurred within the first 10 km below the dam as it was also the case for CH<sub>4</sub>  
421 (Deshmukh et al., 2016). The annual average diffusive CO<sub>2</sub> fluxes were  $126 \pm 137$  and  
422  $288 \pm 346 \text{ mmol m}^{-2} \text{ d}^{-1}$  in 2010 and 2011 respectively. The annual average diffusive CO<sub>2</sub> flux  
423 was one order of magnitude lower in 2013 ( $24 \pm 68 \text{ mmol m}^{-2} \text{ d}^{-1}$ ) (not show). The total  
424 emissions by diffusion and degassing resulting from these fluxes ranged between  $5.5 \pm 0.1$   
425  $\text{Gg(CO}_2\text{) year}^{-1}$  in 2010 and  $0.14 \pm 0.06 \text{ Gg(CO}_2\text{) year}^{-1}$  in 2013 (Figure 6b).

426 On a yearly basis, emissions downstream of NT2R decreased from  $99.7 \pm 25.3$  to  $15.0 \pm 6.5$   
427  $\text{Gg}(\text{CO}_2) \text{ y}^{-1}$  between 2010 and 2013 (Figure 6b). Before the reservoir commissioning in  
428 2009, emissions were dominated by degassing due to spillway releases. After the  
429 commissioning, emissions were dominated by degassing in the downstream channel which  
430 contributed 80-90% of total downstream emissions.

### 431 **3.6 CO<sub>2</sub> bubbling**

432 The CO<sub>2</sub> content in the sampled bubbles was  $0.29 \pm 0.37\%$  (n=2334). On average, the CO<sub>2</sub>  
433 bubbling was  $0.16 \pm 0.24 \text{ mmol m}^{-2} \text{ d}^{-1}$  ( $0-2.8 \text{ mmol m}^{-2} \text{ d}^{-1}$ ) for depth shallower than 16m.  
434 Considering the water surface variations, the monthly ebullitive CO<sub>2</sub> emissions ranged from  
435  $0.04 \pm 0.06$  to  $0.11 \pm 0.16 \text{ Gg}(\text{CO}_2) \text{ month}^{-1}$ . CO<sub>2</sub> bubbling was constant around  $1.1 \pm 2.2$   
436  $\text{Gg}(\text{CO}_2) \text{ y}^{-1}$  throughout the monitoring.

### 437 **3.7 CO<sub>2</sub> emissions from the drawdown area**

438 Four types of pristine soils were identified in the six different studied catenae. Acrisols were  
439 the most represented soils and were found at three sites (RES4S, RES8S and RES8'S) (Table  
440 1). In the area with dense forest, soils were characterized as plinthosol (RES3S) and plinthic  
441 ferralsol (RES2S) and the pedological cover at MNR site belong to planosol type soil (Table  
442 1). At all sites, from upland pristine soils to the shoreline, stagnic properties were more and  
443 more pronounced. Average organic carbon content (%C), nitrogen (%N) and C:N ratio were  
444  $1.84 \pm 0.10\%$ ,  $0.14 \pm 0.01\%$  and  $12.83 \pm 0.30$ , in surface horizons, respectively. For those three  
445 parameters, no statistical differences were obtained according to soil type, topography or  
446 measurement site. Diffusive CO<sub>2</sub> fluxes ranged between  $34 \pm 7$  and  $699 \pm 59 \text{ mmol m}^{-2} \text{ d}^{-1}$   
447 (Table 2). The fluxes were not significantly correlated with the surface moisture (17.5 to  
448 51.2%) and temperature (18.1 to 34.2°C) (Table 2). The fluxes neither varied significantly  
449 with soil types, topography, measurement sites, nitrogen content or C:N ratio ( $p > 0.05$ ,  
450 ANOVA test). However, average fluxes at each site were significantly correlated with the  
451 average C content ( $p=0.0452$ ). Since we did not observe significant spatial variations related  
452 to topography, humidity or temperature that could have been considered for refine spatial and  
453 temporal extrapolation, we further consider the average of all fluxes that is  $279 \pm 27 \text{ mmol m}^{-2}$   
454  $\text{d}^{-1}$  throughout the years.

455 After the commissioning of the reservoir, emissions varied by three orders of magnitude.  
456 Since a constant CO<sub>2</sub> emission is accounted for, the seasonal pattern of CO<sub>2</sub> emission from  
457 the drawdown mimics the variation of the surface of that area (Figure 7). Monthly CO<sub>2</sub>  
458 emissions have reached up to 110.8±10.7 Gg(CO<sub>2</sub>) month<sup>-1</sup> by the end of the WD season  
459 when drawdown area reached its maximum whereas it decreased down to 0.6±0.1 Gg(CO<sub>2</sub>)  
460 month<sup>-1</sup> at the end of WW season when drawdown area reached its minimum (Figure 7).  
461 Around 80-90% of the annual emissions occurred within 4-6 months of transition period  
462 between the WD and WW seasons (Figure 7) when the drawdown area surface is at its  
463 maximum. The lowest emissions from the drawdown area occurred during the wet year 2011  
464 (386±16 Gg(CO<sub>2</sub>) year<sup>-1</sup>) and the highest emissions during the dry year 2012 (572±20  
465 Gg(CO<sub>2</sub>) year<sup>-1</sup>). On average from 2009 to 2013, emissions from the drawdown area was  
466 431±42 Gg(CO<sub>2</sub>) year<sup>-1</sup>.

## 467 **4 Discussion**

### 468 **4.1 CO<sub>2</sub> dynamic in the NT2R water column and downstream rivers**

469 The dynamics of CO<sub>2</sub> in the NT2R is highly dependent on the hydrology and hydrodynamics  
470 of the reservoir as it has already been described for CH<sub>4</sub> (Guérin et al., 2016). During the  
471 warm seasons (WD and WW) when the water column is thermally stratified, the vertical  
472 profiles of CO<sub>2</sub> concentration in the water column are similar to profiles obtained in other  
473 tropical or subtropical reservoirs (Abril et al., 2005;Guérin et al., 2006;Kemenes et al.,  
474 2011;Chanudet et al., 2011) but also boreal reservoirs (Demarty et al., 2011). The high  
475 concentrations measured in the hypolimnion suggest that the main source of CO<sub>2</sub> is located at  
476 the bottom and very likely in the flooded soils, vegetation and sediments whereas the decrease  
477 of CO<sub>2</sub> toward the surface suggest both consumption by primary production and/or loss to the  
478 atmosphere (Galy-Lacaux et al., 1997b;St Louis et al., 2000;Abril et al., 2005;Guérin et al.,  
479 2008;De Junet et al., 2009;Teodoru et al., 2011;Barros et al., 2011;Chanudet et al., 2011). In  
480 the CD season, after the reservoir overturn, the average CO<sub>2</sub> concentration in the reservoir  
481 water column decreases sharply (by 50% on average) and CO<sub>2</sub> concentration increases  
482 regularly from the surface to the bottom of the water column. However, no CO<sub>2</sub> burst was  
483 observed at the beginning of the CD season evidencing that reservoir overturn has only a  
484 moderate impact on CO<sub>2</sub> emissions. This assumption is reinforced by the fact that during the  
485 same sampling, hot moments of CH<sub>4</sub> emissions that should have occurred at the same time  
486 were captured (Guérin et al., 2016). As observed in most tropical and subtropical reservoirs,



487 the higher concentrations were observed during the warm seasons due to long residence time of  
488 water and warmer conditions enhancing CO<sub>2</sub> build-up (Abril et al., 2005;Kemenes et al.,  
489 2011;Chanudet et al., 2011) whereas the lowest were found after reservoir overturn when the  
490 water outgassed (Chanudet et al., 2011). A significant shift in the carbon biogeochemical  
491 cycling occurred in the reservoir in 2013 with the reservoir water surface becoming of CO<sub>2</sub>  
492 sink during the WD season and the beginning of the WW season (from March to August).  
493 Although no major change was observed in nutrient concentrations, the number of  
494 phytoplanktonic cell was 50% higher in 2013 than 2012 (Unpublished, M Cottet personal  
495 com.) indicating that primary production was significantly enhanced in 2013. Despite the fact  
496 that the reservoir was a sink for the six months when CO<sub>2</sub> emissions are usually the highest of  
497 the year, annual CO<sub>2</sub> emissions at the surface of the reservoir were only 50% lower in 2013  
498 than in 2012. In 2013, CO<sub>2</sub> was mainly emitted in the CD after the period of high biological  
499 productivity suggesting that the degradation of autochthonous OM fuels CO<sub>2</sub> emissions.

500 The maximum concentration and the highest CO<sub>2</sub> stock in the water column highly depend on  
501 the age of the reservoir. In the NT2R, average CO<sub>2</sub> concentration was three times higher in  
502 2010 than in 2013 and the maximum concentrations in 2010 was almost two times higher than  
503 in 2013 (4771 μmol L<sup>-1</sup> in 2010 vs. 2649 μmol L<sup>-1</sup> in 2013). Those high concentrations are  
504 slightly lower than the maximum concentration measured in the hypolimnion of the Petit Saut  
505 Reservoir less than a year after it was flooded (Galy-Lacaux et al., 1997a;Abril et al., 2005).  
506 Disregarding these high concentrations observed in the hypolimnion of the reservoir at the  
507 end of the WD season and beginning of the WW season in 2009 and 2010, the CO<sub>2</sub>  
508 concentration in the NT2R are in the same range as concentrations in other older reservoirs in  
509 the tropics or the subtropics (Abril et al., 2005;Guérin et al., 2006;Chanudet et al.,  
510 2011;Kemenes et al., 2011). This decrease during the first four years after impoundment is  
511 very consistent with the decrease of the CO<sub>2</sub> concentration with the reservoir age as already  
512 observed at the Petit Saut Reservoir (Abril et al., 2005), at the Eastmain I Reservoir (Teodoru  
513 et al., 2012) or over multi-sites study (Barros et al., 2011).

514 Disregarding the station RES9 located at the water intake, no significant spatial variation of  
515 CO<sub>2</sub> surface concentrations was found despite very significant differences of hypolimnic  
516 concentration between stations located upstream of the Nakai Dam (RES1, 2 and 3) and  
517 station located in areas close to the three main tributaries (RES6, 7 and 8). The average  
518 hypolimnic concentrations at the stations RES1-3 were two times higher than at the stations

519 RES6-8. This difference is attributed to both (1) the difference in carbon density at the bottom  
520 of the reservoir in those two contrasted areas in terms of submerged ecosystems (Descloux et  
521 al., 2011) (see section 4.3) and (2) the difference in terms of water residence time between  
522 those two zones (Guérin et al., 2016). Stations RES1-3 are located in areas with the longest  
523 water residence time in the reservoir since the water mostly enters the reservoir in the RES6-8  
524 area from the Nam Theun, Nam Noy and Nam On Rivers before being delivered to the water  
525 intake (close to RES9) on the opposite side of NT2R which has a narrow and elongated shape  
526 (Figure 1). Therefore, the water renewal in the RES6-9 area is high and CO<sub>2</sub> accumulates less  
527 in the water column confirming the importance of the reservoir hydrology on the spatial  
528 variability of dissolved gases in reservoirs (Pacheco et al., 2015;Guérin et al., 2016).

529 As found for CH<sub>4</sub>, the main factor influencing the spatial variability of CO<sub>2</sub> in the water  
530 column is the vertical mixing of the water column induced by the water intake located close to  
531 RES9 (Deshmukh et al., 2016;Guérin et al., 2016). The design of the water intake enhances  
532 horizontal water current velocities and vertical mixing which lead to the transport of bottom  
533 waters to the surface. As a consequence, surface concentrations at RES9 were up to 30 times  
534 higher than at other stations in 2010 and 2011 (Figure 5b). With the significant decrease of  
535 concentrations in 2012 and 2013, the difference with other stations dropped to a factor of  
536 four. These maximum surface concentrations at RES9 are up to 10 times higher than  
537 concentrations found in other tropical reservoir in South America (Abril et al., 2005;Guérin et  
538 al., 2006;Kemenes et al., 2011) and Lao PDR (Chanudet et al., 2011) showing that, as for  
539 CH<sub>4</sub>, CO<sub>2</sub> emissions can be enhanced upstream of water intake or dams.

540 Downstream of the reservoir in the Nam Theun River or the artificial channel, CO<sub>2</sub>  
541 concentrations follow the same seasonality as in the reservoir. Concentrations peak in June-  
542 July at the transition between the WD and the WW season, and reach their minima in the CD  
543 season. Downstream of the Nakai Dam, the concentrations are twice lower than downstream  
544 of the powerhouse since mostly epilimnic water from the RES1 station is transferred  
545 downstream of the dam. Within less than 10 km further downstream, concentrations are not  
546 significantly different than in pristine rivers of the watershed. Downstream of the  
547 powerhouse, CO<sub>2</sub> concentrations in 2010 were in the same order of magnitude as in 10-20  
548 years-old reservoirs in South America flooding tropical forest (Abril et al., 2005;Guérin et al.,  
549 2006;Kemenes et al., 2011) whereas four years after impoundment CO<sub>2</sub> concentrations were  
550 two times lower than in 20-30 years-old reservoirs in Lao PDR (Chanudet et al., 2011). We

551 hypothesize that the low CO<sub>2</sub> concentration downstream of the NT2R result from a significant  
552 degassing of the water at the water intake before the water is transferred downstream as  
553 observed for CH<sub>4</sub> (Deshmukh et al., 2016;Guérin et al., 2016).

#### 554 **4.2 Total CO<sub>2</sub> emissions from the Nam Theun 2 Reservoir**

555 From 2009 to 2013, total CO<sub>2</sub> emissions from NT2R show the same seasonal pattern (Figure  
556 8a). The lowest total emissions occur in the CD season while the highest emissions occur at  
557 the transition between the WD and the WW season when emissions by all individual  
558 pathways reach their maximum. From 2010 to 2013, emissions at the transition between the  
559 WD and the WW seasons (April-July) contributed 47 to 61% of total annual emissions  
560 suggesting that quantification of emissions based on two to four campaigns in a year might be  
561 subject to caution since seasonality of emissions significantly affects emission factors.

562 CO<sub>2</sub> bubbling follows the same seasonal variations, being triggered by water level and  
563 concomitant hydrostatic decrease as for CH<sub>4</sub> (Chanton et al., 1989;Engle and Melack,  
564 2000;Smith et al., 2000;Boles et al., 2001;Deshmukh et al., 2014) but its contribution is  
565 negligible (<1%, Table 3). Low CO<sub>2</sub> emission by bubbling as also observed in temperate  
566 reservoirs (Bevelhimer et al., 2016) is attributed to the higher solubility of CO<sub>2</sub> in water than  
567 CH<sub>4</sub> which lead to the solubilisation of the majority of CO<sub>2</sub> as free CO<sub>2</sub> or as DIC.

568 The relative contribution of emissions downstream of the reservoir by degassing and diffusion  
569 from rivers and channels at NT2R are low as compared to most of the reservoirs that were  
570 studied (Abril et al., 2005;Guérin et al., 2006;Kemenes et al., 2011;Bevelhimer et al., 2016)  
571 but the contribution of this pathway is comparable to what was observed in boreal reservoirs  
572 (Roehm and Tremblay, 2006) or in monomictic reservoirs from Lao PDR (Chanudet et al.,  
573 2011). The downstream emissions contributed between 11% at the maximum in the wet 2011  
574 year down to 3% at the minimum in 2013 (Table 3 and Figure 8a). As for CH<sub>4</sub> at NT2R  
575 (Deshmukh et al., 2016), the low downstream emissions are attributed to the significant  
576 degassing at the water intake (station RES9) before the water reach the turbines and to the  
577 flush of CO<sub>2</sub> due to the reservoir overturn in the CD season.

578 Emissions by diffusive fluxes at the surface of the reservoir increased by a factor of two by  
579 the end of the WD season (Figure 5a) compare to the CD season from 2009 to 2012. The  
580 average CO<sub>2</sub> emissions in 2009 and 2010 and in a lesser extend 2011 are in the same range as  
581 emissions from the Petit Saut Reservoir during the first five years after impoundment (Abril et

582 al., 2005) and in the upper range of average CO<sub>2</sub> diffusive fluxes measured in older tropical  
583 reservoirs (dos Santos et al., 2006;Kemenes et al., 2011;Yang et al., 2013) or in young boreal  
584 reservoirs (Teodoru et al., 2011;Tadonl  k   et al., 2012). In 2012 and 2013, emissions from  
585 NT2R by diffusive fluxes are still higher than most of the older Asian reservoirs (Wang et al.,  
586 2011;Chanudet et al., 2011;Zhao et al., 2013;Xiao et al., 2013;Panneer Selvam et al., 2014)  
587 and other Brazilian reservoirs flooding savannah (Roland et al., 2010;Pacheco et al., 2015).  
588 The low emissions in the CD season from the first 3.5 years might mostly result from lower  
589 heterotrophic activity due to the low temperature (down to 7  C in air in March 2011). The  
590 high emissions in the CD season of 2013 as compared to CD season in 2011 and 2012 likely  
591 to be originated from additional autochthonous OM. We hypothesise that the significantly  
592 higher CO<sub>2</sub> emissions in the WD season result from the increase of the water residence time  
593 that favour CO<sub>2</sub> accumulation in the water column (Abril et al., 2005) and the increase of  
594 temperature that enhance aerobic and anaerobic degradation of OM and the production of CO<sub>2</sub>  
595 (Sobek et al., 2005). Although the reservoir area during the WD season is the smallest of the  
596 year, emissions by diffusive fluxes are the highest (Figure 8a) highlighting the very  
597 significant increase of CO<sub>2</sub> emissions from May to July every year, disregarding the year  
598 2013.

599 This first estimation of the CO<sub>2</sub> emission from the drawdown area to the total emission from a  
600 reservoir reveal that with a contribution ranging from 40 to more than 75%, it could be a  
601 major CO<sub>2</sub> pathway to the atmosphere. These results from the NT2R cannot be generalized to  
602 all reservoirs since its contribution is tightly link to the very high-water level variations and  
603 large surface area of the drawdown area (up to 320 km<sup>2</sup>, Figure 7). However, areal fluxes  
604 from the drawdown area are on average 2.5 times higher than the diffusive fluxes from the  
605 reservoir water surface in 2009-2010 and six times higher than those fluxes in 2013 making  
606 the soils in the area of influence of the reservoir a hotspot for CO<sub>2</sub> emissions compare to the  
607 reservoir surface waters. The total emissions of reservoirs with contrasted hydrology  
608 characterized by marked wet and dry seasons and large water level variations of 30% of the  
609 total surface could have been significantly underestimated as it is the case for Petit Saut (~100  
610 km<sup>2</sup>), Samuel (~280 km<sup>2</sup>), Balbina (~220 km<sup>2</sup>) or Three Gorges Reservoir (~400 km<sup>2</sup>) for  
611 instance (Gu  rin et al., 2006;Kemenes et al., 2011;Li et al., 2016). This pathway is expected  
612 to be more significant in flat bottom reservoirs than in valley type reservoirs in mountainous  
613 regions and cannot be generalized on just the drawdown area without taking into account  
614 hydrological water management and the local topography. At Petit Saut and NT2R at least, no

615 vegetation regrowth occurs in the drawdown areas. Soils at NT2R exhibit very clear  
616 modification related to the flooding (stagnic features) confirming soil modification as also  
617 observed in Canada (Furey et al., 2004) Australia (Watts, 2000) and France (Félix-Faure et  
618 al., 2017). The ecosystems of the seasonally flooded area are therefore significantly modified  
619 and CO<sub>2</sub> emissions from the drawdown must be accounted for in total gross emissions from  
620 reservoirs. Although drawdown emissions cannot be neglected in terms of gross CO<sub>2</sub>  
621 exchange, the emissions resulting from the soil respiration are currently comparable to  
622 pristine emissions (Table 2) and the impact of these area in terms of net emissions requires  
623 further specific studies in these overlooked ecosystems (Prairie et al., 2017). So far, we cannot  
624 predict future evolution of CO<sub>2</sub> emissions in this area based on the available data. The  
625 consequence of the flooding on the respiration rate of these soils may lead to a decrease of  
626 emissions with time or a stabilization (see next section). Therefore, the net contribution of the  
627 drawdown zone to emissions from the reservoir remains unclear and specifically requires  
628 research on soil OM dynamics and would also require the inclusion of the vegetation  
629 dynamics when present.

630 This is the first comprehensive quantification of CO<sub>2</sub> emissions from a reservoir where all  
631 known CO<sub>2</sub> pathways to the atmosphere were taken into account at one of the best spatial and  
632 temporal resolution reported in the literature. We showed that downstream emissions and  
633 emissions around the water intake are not negligible (~10% overall) and that the overlooked  
634 drawdown area in CO<sub>2</sub> studies could be the main emission pathway of CO<sub>2</sub> to the atmosphere.  
635 Overall, this study highlights that global estimate of CO<sub>2</sub> emissions from reservoir are  
636 underestimated so far since relevant pathways like drawdown emissions in flat/shallow  
637 reservoirs with large water level variations and downstream emissions in thermally stratified  
638 reservoirs are missing in most site-specific studies used for extrapolations (Deemer et al.,  
639 2016;Barros et al., 2011).

#### 640 **4.3 Source of organic matter fuelling the reservoir CO<sub>2</sub> emissions**

641 In tropical reservoirs, the decrease of the CO<sub>2</sub> concentration in the water column and  
642 subsequent emissions with the age of the reservoir (Figure 8b) is supposed to result from the  
643 decrease of the aerobic and anaerobic mineralisation rate due to the exhaustion of labile OM  
644 from the pool of soil and vegetation that was flooded during impoundment (Abril et al.,  
645 2005;Guérin et al., 2008). In boreal reservoirs, the decrease of benthic CO<sub>2</sub> production is

646 sharp and after 3-5 years, most of the CO<sub>2</sub> production appears to be pelagic and is supposed  
647 not to result from the flooded organic matter (Teodoru et al., 2011;Brothers et al., 2012). The  
648 total CO<sub>2</sub> emissions were nine and three times higher than the carbon inputs from the  
649 watershed to the NT2R in 2010 (32 GgC yr<sup>-1</sup>) and 2013 (45 GgC yr<sup>-1</sup>), respectively (Figure 3  
650 and Table 3). It has to be noted that interannual variations of carbon inputs to the NT2R  
651 (Figure 3) are not correlated with the regular decrease of total CO<sub>2</sub> emissions from year to  
652 year (Figure 8b). It is therefore unlikely that most of CO<sub>2</sub> emissions result from the  
653 mineralization of allochthonous OM but rather from the contribution of the flooded carbon  
654 pool (soil and vegetation) which amount is decreasing with time. This is consistent with the  
655 fact that at Petit Saut, even 10 years after flooding, the majority of the OM in the water  
656 column has a terrestrial origin (De Junet et al., 2009). According to Abril et al. (2005) at Petit  
657 Saut, total emissions (disregarding drawdown emissions which were not measured) were 9 to  
658 6 times higher than carbon inputs from the watershed during the first 4 years for similar  
659 carbon inputs which indicates a faster decrease of emissions in NT2R than at Petit Saut. This  
660 sharp decrease of emissions at NT2R might be due to the fact that the flooded pool of OM and  
661 therefore the amount of labile OM in NT2R was twice smaller than the amount of OM  
662 flooded in the Petit Saut (Guérin et al., 2008;Descloux et al., 2011). We show here, as it was  
663 done at Petit Saut (Guérin et al., 2008;Abril et al., 2005), that external sources of carbon are  
664 not sufficient to fuel the CO<sub>2</sub> emissions from the NT2R and we attribute the decrease of  
665 emissions with time to the exhaustion of the most labile fraction of the flooded pool of OM  
666 which might be the main source of reactive carbon in the reservoir.

667 In the sub-tropical NT2R, CO<sub>2</sub> concentrations are always higher at the bottom than in the  
668 epilimnic waters even during the CD season when the limited thermal stratification or its  
669 absence do not favour hypolimnic CO<sub>2</sub> accumulation. The CD season is probably the most  
670 favourable season to pelagic respiration as this process is enhanced by the re-oxygenation of  
671 the water column (Bastviken et al., 2004). Since CO<sub>2</sub> concentration in the CD season is 50%  
672 lower than in the warm seasons, we suggest that CO<sub>2</sub> is mostly produced in the sediment and  
673 flooded soils and vegetation. Disregarding the station RES9 located at the water intake,  
674 significant spatial variation of CO<sub>2</sub> hypolimnic concentrations were found between stations  
675 located in the area of dense forest (RES1-3) versus stations located in areas close to the three  
676 main tributaries (RES6-8). Stations RES1-3 which have the highest average bottom  
677 concentrations are located in areas where the carbon density is 50% higher than the

678 agricultural ecosystems that were flooded in the area of the stations RES6-8 (Descloux et al.,  
679 2011).

680 In the absence of significant vegetation regrowth in the drawdown area during the study  
681 period, the main source of carbon fuelling emissions from the drawdown area are not clearly  
682 identified. Immediately after flooding, the most labile part of the soil OM and the  
683 decomposing vegetation must have been the main sources of C fuelling the emissions. On the  
684 long haul, the atmospheric carbon sink associated with the pristine vegetation dynamics has  
685 been lost but as a consequence, the loss of this vegetation which might reduce labile OM  
686 inputs. In addition, the water level variations erode the soil and OM is transferred to the  
687 reservoir and ultimately in the sediments or downstream (Félix-Faure et al., 2017). Those  
688 carbon losses should have resulted or should result in the future in a decrease of CO<sub>2</sub>  
689 emissions from the drawdown. The stability of emissions throughout our four-years surveys  
690 in the drawdown area suggests that new carbon source might have contributed to emissions.  
691 Development of micro-phytobenthos or microbial biofilms as often observed in estuaries on  
692 mudflats (de Brouwer and Stal, 2001) or along stream in logged riparian area (Sabater et al.,  
693 2000) could supply labile OM to the system and favour priming effect (Guenet et al., 2010).  
694 Through this effect, the inputs of labile OM stimulate the degradation/mineralization of  
695 recalcitrant/stabilized OM. This effect might be enhanced by the oxic/anoxic oscillation that  
696 would favour the mineralisation of different pool of OM than those that would have been  
697 degraded otherwise in stable conditions (Abril et al., 1999; Bastviken et al., 2004). Overall, we  
698 hypothesized that the oxic/anoxic variations and priming effect through the development of  
699 algae and bacteria might have contributed to the stability of CO<sub>2</sub> emission from these soils  
700 under the influence of the reservoir. So far we found no clear evidence of a significant carbon  
701 loss in the soils of the drawdown area by comparing surface SOM from pristine upland soils  
702 and from the shoreline (Table 1). A comprehensive study of carbon density down to the  
703 bedrock would be necessary since we found very clear evidence of inundation patterns down  
704 to 1 m (P. Oliva, unpublished). In addition to the full carbon stock, detailed OM  
705 characterisation might be needed for the identification of changes in the pool of soil OM.

706 The overall confirmation of the importance of the flooded pool of OM in the carbon cycling  
707 in a tropical reservoir highlights the differences in functioning with boreal reservoirs where  
708 the degradation of the flooded organic matter within a few year does not contribute  
709 significantly to emissions (Brothers et al., 2012). In addition to a strong temperature effect on

710 mineralisation of OM (Gudasz et al., 2010), the probable low lability and good capacity for  
711 preservation of peat-dominated OM might explain the different origin of OM fuelling  
712 emissions between those two distinct climatic areas.

## 713 **5 Conclusions**

714 We presented the first comprehensive estimation of CO<sub>2</sub> emissions from a subtropical  
715 reservoir starting less than a year after reservoir impoundment and lasting 4.5 years. This  
716 estimation includes all known pathways to the atmosphere: emissions from the reservoir  
717 surface, downstream emissions and emissions from the drawdown area.

718 More than 50% of total emissions occur within 3-4 months during the warmest period of the  
719 year at the transition between the dry and the wet season. Such a result suggests that  
720 quantification of emissions based on two to four campaigns in a year might significantly  
721 affect positively or negatively emissions factors and carbon budgets of ecosystems under  
722 study.

723 The smooth decrease of total emissions over the years coupled with the fact that the incoming  
724 flux of carbon from the watershed to the reservoir represents less than a third of the total  
725 emissions, are a strong indication that the flooded pool of organic matter is the main source of  
726 carbon fuelling emissions. The carbon density of flooded soil and biomass in reservoirs  
727 appears to be a key controlling factor of emissions and should be included for future  
728 estimation of greenhouse gas emissions from reservoirs.

729 We found that gross CO<sub>2</sub> emissions from the drawdown area represented 40- 75% of the total  
730 emissions from the NT2R and they occur within a few months during low water level seasons.  
731 The soil organic matter from these areas undergoes anaerobic degradation and fuels the  
732 reservoir water column in CO<sub>2</sub> during the wet season. In the dry season, the soil loss CO<sub>2</sub>  
733 directly to the atmosphere while undergoing both aerobic and anaerobic mineralisation  
734 depending on the soil moisture content. We hypothesize that both (1) the potential  
735 development of bacteria and micro-phytobenthos at the surface of these soils and (2) the  
736 oxic/anoxic variations contribute to the mineralisation of stabilized SOM leading to a  
737 sustained high soil respiration even after the pristine vegetation decayed. This overlooked  
738 pathway in terms of gross emissions would require an in-depth evaluation for the soil OM and  
739 vegetation dynamics and long-term monitoring of emissions to evaluate the real contribution  
740 of this area in terms of net modification of gas exchange in the footprint of the reservoir.



741 **Acknowledgements**

742 The authors thank everyone who contributed to the NT2 monitoring programme, especially  
743 the Nam Theun 2 Power Company (NTPC), Electricité de France (EDF) and CNRS-INSU  
744 (Submersoil project, EC2CO-BIOHEFECT) for providing financial, technical and logistic  
745 support. We are also grateful to the Aquatic Environment Laboratory of the Nam Theun 2  
746 Power Company whose Shareholders are EDF, Lao Holding State Enterprise and Electricity  
747 Generating Public Company Limited of Thailand. CD benefited from a PhD grant by EDF.  
748

750 **References**

- 751 Abril, G., Etcheber, H., Le Hir, P., Bassoullet, P., Boutier, B., and Frankignoulle, M.:  
 752 Oxic/anoxic oscillations and organic carbon mineralization in an estuarine maximum turbidity  
 753 zone (The Gironde, France), *Limnology and Oceanography*, 44, 1304-1315, 1999.
- 754 Abril, G., Guérin, F., Richard, S., Delmas, R., Galy-Lacaux, C., Gosse, P., Tremblay, A.,  
 755 Varfalvy, L., Dos Santos, M. A., and Matvienko, B.: Carbon dioxide and methane emissions  
 756 and the carbon budget of a 10-year old tropical reservoir (Petit Saut, French Guiana), *Global*  
 757 *Biogeochem. Cycles*, 19, 10.1029/2005gb002457, 2005.
- 758 Abril, G., Commarieu, M.-V., and Guérin, F.: Enhanced methane oxidation in an estuarine  
 759 turbidity maximum, *Limnol. Oceanogr.*, 52, 470-475, 2007.
- 760 Barros, N., Cole, J. J., Tranvik, L. J., Prairie, Y. T., Bastviken, D., Huszar, V. L. M., del  
 761 Giorgio, P., and Roland, F.: Carbon emission from hydroelectric reservoirs linked to reservoir  
 762 age and latitude, *Nature Geosci*, 4, 593-596, 2011.
- 763 Bastviken, D., Persson, L., Odham, G., and Tranvik, L.: Degradation of dissolved organic  
 764 matter in oxic and anoxic lake water, *Limnology and Oceanography*, 49, 109-116, 2004.
- 765 Bevelhimer, M., Stewart, A., Fortner, A., Phillips, J., and Mosher, J.: CO<sub>2</sub> is Dominant  
 766 Greenhouse Gas Emitted from Six Hydropower Reservoirs in Southeastern United States  
 767 during Peak Summer Emissions, *Water*, 8, 15, 2016.
- 768 Boles, J. R., Clark, J. F., Leifer, I., and Washburn, L.: Temporal variation in natural methane  
 769 seep rate due to tides, Coal Oil Point area, California, *Journal of Geophysical Research:*  
 770 *Oceans*, 106, 27077-27086, 10.1029/2000JC000774, 2001.
- 771 Brothers, S. M., Prairie, Y. T., and del Giorgio, P. A.: Benthic and pelagic sources of carbon  
 772 dioxide in boreal lakes and a young reservoir (Eastmain-1) in eastern Canada, *Global*  
 773 *Biogeochem. Cycles*, 26, GB1002, 10.1029/2011gb004074, 2012.
- 774 Chanton, J. P., Martens, C. S., and Kelley, C. A.: Gas Transport from Methane-Saturated,  
 775 Tidal Freshwater and Wetland Sediments, *Limnology and Oceanography*, 34, 807-819, 1989.
- 776 Chanudet, V., Descloux, S., Harby, A., Sundt, H., Hansen, B. H., Brakstad, O., Serca, D., and  
 777 Guérin, F.: Gross CO<sub>2</sub> and CH<sub>4</sub> emissions from the Nam Ngum and Nam Leuk sub-tropical  
 778 reservoirs in Lao PDR, *Sci. Total Environ.*, 409, 5382-5391, 10.1016/j.scitotenv.2011.09.018,  
 779 2011.
- 780 Chanudet, V., Fabre, V., and van der Kaaij, T.: Application of a three-dimensional  
 781 hydrodynamic model to the Nam Theun 2 Reservoir (Lao PDR), *J. Great Lakes Res.*, 38, 260-  
 782 269, <http://dx.doi.org/10.1016/j.jglr.2012.01.008>, 2012.
- 783 Chen, H., Wu, Y., Yuan, X., Gao, Y., Wu, N., and Zhu, D.: Methane emissions from newly  
 784 created marshes in the drawdown area of the Three Gorges Reservoir, *J. Geophys. Res.*, 114,  
 785 D18301, doi:10.1029/2009JD012410, 2009.
- 786 Chen, H., Yuan, X., Chen, Z., Wu, Y., Liu, X., Zhu, D., Wu, N., Zhu, Q. a., Peng, C., and Li,  
 787 W.: Methane emissions from the surface of the Three Gorges Reservoir, *J. Geophys. Res.*,  
 788 116, D21306, 10.1029/2011jd016244, 2011.

789 de Brouwer, J. F. C., and Stal, L. J.: Short-term dynamics in microphytobenthos distribution  
790 and associated extracellular carbohydrates in surface sediments of an intertidal mudflat,  
791 *Marine Ecology Progress Series*, 218, 33-44, 2001.

792 De Junet, A., Abril, G., Guérin, F., Billy, I., and De Wit, R.: A multi-tracers analysis of  
793 sources and transfers of particulate organic matter in a tropical reservoir (Petit Saut, French  
794 Guiana), *River Research and Applications*, 25, 253-271, 10.1002/rra.1152, 2009.

795 Deemer, B. R., Harrison, J. A., Li, S., Beaulieu, J. J., DelSontro, T., Barros, N., Bezerra-Neto,  
796 J. F., Powers, S. M., dos Santos, M. A., and Vonk, J. A.: Greenhouse Gas Emissions from  
797 Reservoir Water Surfaces: A New Global Synthesis, *BioScience*, 10.1093/biosci/biw117,  
798 2016.

799 Demarty, M., Bastien, J., and Tremblay, A.: Annual follow-up of gross diffusive carbon  
800 dioxide and methane emissions from a boreal reservoir and two nearby lakes in Québec,  
801 Canada, *Biogeosciences*, 8, 41-53, 10.5194/bg-8-41-2011, 2011.

802 Descloux, S., Chanudet, V., Poilvé, H., and Grégoire, A.: Co-assessment of biomass and soil  
803 organic carbon stocks in a future reservoir area located in Southeast Asia, *Environ. Monit.*  
804 *Assess.*, 173, 723-741, 10.1007/s10661-010-1418-3, 2011.

805 Descloux, S., Guedant, P., Phommachanh, D., and Luthi, R.: Main features of the Nam Theun  
806 2 hydroelectric project (Lao PDR) and the associated environmental monitoring programmes,  
807 *Hydroécol. Appl.*, 19, 5-25, 2016.

808 Deshmukh, C., Serca, D., Delon, C., Tardif, R., Demarty, M., Jarnot, C., Meyerfeld, Y.,  
809 Chanudet, V., Guedant, P., Rode, W., Descloux, S., and Guérin, F.: Physical controls on CH<sub>4</sub>  
810 emissions from a newly flooded subtropical freshwater hydroelectric reservoir: Nam Theun 2,  
811 *Biogeosciences*, 11, 4251-4269, 10.5194/bg-11-4251-2014, 2014.

812 Deshmukh, C., Guérin, F., Labat, D., Pighini, S., Vongkhamsao, A., Guédant, P., Rode, W.,  
813 Godon, A., Chanudet, V., Descloux, S., and Serça, D.: Low methane (CH<sub>4</sub>) emissions  
814 downstream of a monomictic subtropical hydroelectric reservoir (Nam Theun 2, Lao PDR),  
815 *Biogeosciences*, 13, 1919-1932, 10.5194/bg-13-1919-2016, 2016.

816 dos Santos, M. A., Rosa, L. P., Sikar, B., Sikar, E., and dos Santos, E. O.: Gross greenhouse  
817 gas fluxes from hydro-power reservoir compared to thermo-power plants, *Energy Policy*, 34,  
818 481-488, 10.1016/j.enpol.2004.06.015, 2006.

819 Engle, D., and Melack, J. M.: Methane emissions from an Amazon floodplain lake: Enhanced  
820 release during episodic mixing and during falling water, *Biogeochemistry*, 51, 71-90, 2000.

821 Félix-Faure, J., Chanudet, V., Walter, C., Dorioz, J.-M., Baudoin, J.-M., Lissolo, T.,  
822 Descloux, S., and Dambrine, E.: Evolution des sols ennoyés sous les retenues de barrage :  
823 Influence sur l'écologie des plans d'eau et la dynamique des gaz à effet de serre, *Etude et*  
824 *Gestion des Sols*, 24, 45-58, 2017.

825 Furey, P. C., Nordin, R. N., and Mazumder, A.: Water Level Drawdown Affects Physical and  
826 Biogeochemical Properties of Littoral Sediments of a Reservoir and a Natural Lake, *Lake and*  
827 *Reservoir Management*, 20, 280-295, 10.1080/07438140409354158, 2004.

828 Galy-Lacaux, C., Delmas, R., Dumestre, J.-F., and Richard, S.: Evolution temporelle des  
829 émissions gazeuses et des profils de gaz dissous Estimation du bilan de carbone de la retenue  
830 de Petit-Saut deux ans après sa mise en eau, *Hydroécol. Appl.*, 9, 85-114, 1997a.

831 Galy-Lacaux, C., Delmas, R., Jambert, C., Dumestre, J. F., Labroue, L., Richard, S., and  
832 Gosse, P.: Gaseous emissions and oxygen consumption in hydroelectric dams: A case study in  
833 French Guyana, *Global Biogeochem. Cycles*, 11, 471-483, 1997b.

834 Gudasz, C., Bastviken, D., Steger, K., Premke, K., Sobek, S., and Tranvik, L. J.:  
835 Temperature-controlled organic carbon mineralization in lake sediments, *Nature*, 466, 478-  
836 481, 2010.

837 Guenet, B., Danger, M., Abbadie, L., and Lacroix, G.: Priming effect: bridging the gap  
838 between terrestrial and aquatic ecology, *Ecology*, 91, 2850-2861, 10.1890/09-1968.1, 2010.

839 Guérin, F., Abril, G., Richard, S., Burban, B., Reynouard, C., Seyler, P., and Delmas, R.:  
840 Methane and carbon dioxide emissions from tropical reservoirs: Significance of downstream  
841 rivers, *Geophys. Res. Lett.*, 33, 10.1029/2006gl027929, 2006.

842 Guérin, F., and Abril, G.: Significance of pelagic aerobic methane oxidation in the methane  
843 and carbon budget of a tropical reservoir, *Journal of Geophysical Research: Biogeosciences*,  
844 112, G03006, 10.1029/2006JG000393, 2007.

845 Guérin, F., Abril, G., Serça, D., Delon, C., Richard, S., Delmas, R., Tremblay, A., and  
846 Varfalvy, L.: Gas transfer velocities of CO<sub>2</sub> and CH<sub>4</sub> in a tropical reservoir and its river  
847 downstream, *Journal of Marine Systems*, 66, 161-172, 2007.

848 Guérin, F., Abril, G., de Junet, A., and Bonnet, M.-P.: Anaerobic decomposition of tropical  
849 soils and plant material: Implication for the CO<sub>2</sub> and CH<sub>4</sub> budget of the Petit Saut Reservoir,  
850 *Appl. Geochem.*, 23, 2272-2283, 10.1016/j.apgeochem.2008.04.001, 2008.

851 Guérin, F., Deshmukh, C., Labat, D., Pighini, S., Vongkhamso, A., Guédant, P., Rode, W.,  
852 Godon, A., Chanudet, V., Descloux, S., and Serça, D.: Effect of sporadic destratification,  
853 seasonal overturn, and artificial mixing on CH<sub>4</sub> emissions from a subtropical hydroelectric  
854 reservoir, *Biogeosciences*, 13, 3647-3663, 10.5194/bg-13-3647-2016, 2016.

855 Kemenes, A., Forsberg, B. R., and Melack, J. M.: CO<sub>2</sub> emissions from a tropical  
856 hydroelectric reservoir (Balbina, Brazil), *J. Geophys. Res.*, 116, G03004,  
857 10.1029/2010jg001465, 2011.

858 Li, Z., Zhang, Z., Lin, C., Chen, Y., Wen, A., and Fang, F.: Soil-air greenhouse gas fluxes  
859 influenced by farming practices in reservoir drawdown area: A case at the Three Gorges  
860 Reservoir in China, *Journal of Environmental Management*, 181, 64-73,  
861 <http://dx.doi.org/10.1016/j.jenvman.2016.05.080>, 2016.

862 Lovatt Smith, P. F., Stokes, R. B., Bristow, C., and Carter, A.: Mid-Cretaceous inversion in  
863 the Northern Khorat Plateau of Lao PDR and Thailand, *Geological Society, London, Special  
864 Publications*, 106, 233-247, 10.1144/gsl.sp.1996.106.01.15, 1996.

865 MacIntyre, S., Jonsson, A., Jansson, M., Aberg, J., Turney, D. E., and Miller, S. D.: Buoyancy  
866 flux, turbulence, and the gas transfer coefficient in a stratified lake, *Geophys. Res. Lett.*, 37,  
867 L24604, 10.1029/2010GL044164, 2010.

868 Marotta, H., Pinho, L., Gudasz, C., Bastviken, D., Tranvik, L. J., and Enrich-Prast, A.:  
869 Greenhouse gas production in low-latitude lake sediments responds strongly to warming,  
870 *Nature Clim. Change*, 4, 467-470, 10.1038/nclimate2222, 2014.

871 Pacheco, F. S., Soares, M. C. S., Assireu, A. T., Curtarelli, M. P., Roland, F., Abril, G., Stech,  
872 J. L., Alvalá, P. C., and Ometto, J. P.: The effects of river inflow and retention time on the  
873 spatial heterogeneity of chlorophyll and water-air CO<sub>2</sub> fluxes in a tropical hydropower  
874 reservoir, *Biogeosciences*, 12, 147-162, 10.5194/bg-12-147-2015, 2015.

875 Panneer Selvam, B., Natchimuthu, S., Arunachalam, L., and Bastviken, D.: Methane and  
876 carbon dioxide emissions from inland waters in India – implications for large scale  
877 greenhouse gas balances, *Global Change Biology*, n/a-n/a, 10.1111/gcb.12575, 2014.

878 Prairie, Y. T., Alm, J., Beaulieu, J., Barros, N., Battin, T., Cole, J., del Giorgio, P., DelSontro,  
879 T., Guérin, F., Harby, A., Harrison, J., Mercier-Blais, S., Serça, D., Sobek, S., and Vachon,  
880 D.: Greenhouse Gas Emissions from Freshwater Reservoirs: What Does the Atmosphere  
881 See?, *Ecosystems*, 10.1007/s10021-017-0198-9, 2017.

882 Raymond, P. A., Hartmann, J., Lauerwald, R., Sobek, S., McDonald, C., Hoover, M.,  
883 Butman, D., Striegl, R., Mayorga, E., Humborg, C., Kortelainen, P., Durr, H., Meybeck, M.,  
884 Ciais, P., and Guth, P.: Global carbon dioxide emissions from inland waters, *Nature*, 503,  
885 355-359, 2013.

886 Roehm, C., and Tremblay, A.: Role of turbines in the carbon dioxide emissions from two  
887 boreal reservoirs, Quebec, Canada, *Journal of Geophysical Research-Atmospheres*, 111,  
888 D24101, 10.1029/2006jd007292, 2006.

889 Roland, F., Vidal, L. O., Pacheco, F. S., Barros, N. O., Assireu, A., Ometto, J., Cimbleiris, A.  
890 C. P., and Cole, J. J.: Variability of carbon dioxide flux from tropical (Cerrado) hydroelectric  
891 reservoirs, *Aquatic Sciences*, 72, 283-293, 10.1007/s00027-010-0140-0, 2010.

892 Sabater, F., Butturini, A., Martí, E., Muñoz, I., Romani, A., Wray, J., and Sabater, S.: Effects  
893 of riparian vegetation removal on nutrient retention in a Mediterranean stream, *Journal of the*  
894 *North American Benthological Society*, 19, 609-620, 10.2307/1468120, 2000.

895 Serça, D., Delmas, R., Jambert, C., and Labroue, L.: Emissions of nitrogen oxides from  
896 equatorial rain forest in central Africa, *Tellus B*, 46, 10.3402/tellusb.v46i4.15795, 1994.

897 Serça, D., Deshmukh, C., Pighini, S., Oudone, P., Vongkhamsoo, A., Guédant, P., Rode, W.,  
898 Godon, A., Chanudet, V., Descloux, S., and Guérin, F.: Nam Theun 2 Reservoir four years  
899 after commissioning: significance of drawdown methane emissions and other pathways,  
900 *Hydroécol. Appl.*, 19, 119-146, 2016.

901 Smith, L. K., Lewis, W. M., Chanton, J. P., Cronin, G., and Hamilton, S. K.: Methane  
902 emissions from the Orinoco River floodplain, Venezuela, *Biogeochemistry*, 51, 113-140,  
903 10.1023/a:1006443429909, 2000.

904 Smith, P. F. L., and Stokes, R. B.: GEOLOGY AND PETROLEUM POTENTIAL OF THE  
905 KHORAT PLATEAU BASIN IN THE VIENTIANE AREA OF LAO P.D.R, *Journal of*  
906 *Petroleum Geology*, 20, 27-49, 10.1111/j.1747-5457.1997.tb00754.x, 1997.

907 Sobek, S., Tranvik, L. J., and Cole, J. J.: Temperature independence of carbon dioxide  
908 supersaturation in global lakes, *Glob. Biogeochem. Cycle*, 19, GB2003,  
909 10.1029/2004gb002264, 2005.

910 St Louis, V. L., Kelly, C. A., Duchemin, E., Rudd, J. W. M., and Rosenberg, D. M.: Reservoir  
911 surfaces as sources of greenhouse gases to the atmosphere: A global estimate, *Bioscience*, 50,  
912 766-775, 2000.

913 Tadonlélé, R. D., Marty, J., and Planas, D.: Assessing factors underlying variation of CO<sub>2</sub>  
914 emissions in boreal lakes vs. reservoirs, *FEMS Microbiology Ecology*, 79, 282-297,  
915 10.1111/j.1574-6941.2011.01218.x, 2012.

916 Teodoru, C. R., Prairie, Y. T., and del Giorgio, P. A.: Spatial Heterogeneity of Surface CO<sub>2</sub>  
917 Fluxes in a Newly Created Eastmain-1 Reservoir in Northern Quebec, Canada, *Ecosystems*,  
918 14, 28-46, 10.1007/s10021-010-9393-7, 2011.

919 Teodoru, C. R., Bastien, J., Bonneville, M.-C., del Giorgio, P. A., Demarty, M., Garneau, M.,  
920 Hélie, J.-F., Pelletier, L., Prairie, Y. T., Roulet, N. T., Strachan, I. B., and Tremblay, A.: The  
921 net carbon footprint of a newly created boreal hydroelectric reservoir, *Global Biogeochem.*  
922 *Cycles*, 26, GB2016, 10.1029/2011gb004187, 2012.

923 Wang, F., Wang, B., Liu, C.-Q., Wang, Y., Guan, J., Liu, X., and Yu, Y.: Carbon dioxide  
924 emission from surface water in cascade reservoirs–river system on the Maotiao River,  
925 southwest of China, *Atmospheric Environment*, 45, 3827-3834,  
926 <http://dx.doi.org/10.1016/j.atmosenv.2011.04.014>, 2011.

927 Watts, C. J.: Seasonal phosphorus release from exposed, re-inundated littoral sediments of  
928 two Australian reservoirs, *Hydrobiologia*, 431, 27-39, 10.1023/a:1004098120517, 2000.

929 Weiss, R. F.: Carbon dioxide in water and seawater: the solubility of a non-ideal gas, *Marine*  
930 *Chemistry*, 2, 203-215, [http://dx.doi.org/10.1016/0304-4203\(74\)90015-2](http://dx.doi.org/10.1016/0304-4203(74)90015-2), 1974.

931 Xiao, S., Wang, Y., Liu, D., Yang, Z., Lei, D., and Zhang, C.: Diel and seasonal variation of  
932 methane and carbon dioxide fluxes at Site Guojiaba, the Three Gorges Reservoir, *Journal of*  
933 *Environmental Sciences*, 25, 2065-2071, [http://dx.doi.org/10.1016/S1001-0742\(12\)60269-1](http://dx.doi.org/10.1016/S1001-0742(12)60269-1),  
934 2013.

935 Yang, L., Lu, F., Wang, X., Duan, X., Song, W., Sun, B., Chen, S., Zhang, Q., Hou, P.,  
936 Zheng, F., Zhang, Y., Zhou, X., Zhou, Y., and Ouyang, Z.: Surface methane emissions from  
937 different land use types during various water levels in three major drawdown areas of the  
938 Three Gorges Reservoir, *Journal of Geophysical Research: Atmospheres*, 117, D10109,  
939 10.1029/2011JD017362, 2012.

940 Yang, L., Lu, F., Wang, X., Duan, X., Tong, L., Ouyang, Z., and Li, H.: Spatial and seasonal  
941 variability of CO<sub>2</sub> flux at the air-water interface of the Three Gorges Reservoir, *Journal of*  
942 *Environmental Sciences*, 25, 2229-2238, [http://dx.doi.org/10.1016/S1001-0742\(12\)60291-5](http://dx.doi.org/10.1016/S1001-0742(12)60291-5),  
943 2013.

944 Yvon-Durocher, G., Allen, A. P., Bastviken, D., Conrad, R., Gudas, C., St-Pierre, A., Thanh-  
945 Duc, N., and del Giorgio, P. A.: Methane fluxes show consistent temperature dependence  
946 across microbial to ecosystem scales, *Nature*, 507, 488-491, 10.1038/nature13164, 2014.

947 Zhao, Y., Wu, B. F., and Zeng, Y.: Spatial and temporal patterns of greenhouse gas emissions  
948 from Three Gorges Reservoir of China, *Biogeosciences*, 10, 1219-1230, 10.5194/bg-10-1219-  
949 2013, 2013.

950

951

Table 1 : Soil type and characteristics at the sampling station of the drawdown area of the Nam Theun 2 Reservoir (Lao PDR). KKK formation.

Catena	solum	%N	%C	C:N	pH	Soil name WRB FAO	Soil texture	lithology
MNR	MNR upland	0.11	1.47	13.69±1.73	4.33	planosol	sandy	Micaceous quartzose
	MNR interm. down	0.10	1.32	13.55±1.84		endogleyic planosol		
	MNR shoreline	0.13	1.89	14.78±1.60	4.23	gleysol		
RES3S	RES3 upland	0.18	2.38	13.21±0.63	4.18	plinthosol	clay	Red mudstone
	RES3 interm.					etagnic plinthosol		
	RES3 shoreline	0.17	1.95	11.21±0.56	4.88	plinthic stagnosol		
RES2S	RES2 upland	0.16	2.24	13.62±0.60		plinthic ferralsol	sandy clay	Micaceous sandstone
	RES2 interm.	0.20	2.30	11.25±0.50		« stagnic » ferralsol		
	RES2 shoreline	0.13	1.41	10.55±0.54		stagnosol		
RES8S	RES8 upland	0.08	1.76	23.47±3.95		acrisol	sandy clay	Quaternary deposits
	RES8 interm. up	0.06	0.68	11.93±1.46		stagnic acrisol		
	RES8 interm. down	0.09	1.31	13.99±1.99		stagnic acrisol		
	RES8 shoreline	0.12	2.02	17.07±1.93		endogleyic stagnosol		
RES8'S	RES8' upland	0.05	0.77	16.15±2.30		acrisol	sandy clay	Quaternary deposits
	RES8' shoreline	0.08	1.51	18.22±2.79		endogleyic stagnosol		
RES4S	RES4 upland	0.16	1.98	12.76±1.17	4.14	acrisol	sandy clay	Micaceous sandstone
	RES4 interm. up	0.13	1.92	14.66±1.58		stagnic acrisol		
	RES4 interm. down	0.12	1.67	14.33±1.71		stagnic acrisol		
	RES4 shoreline	0.10	1.36	14.35±1.97	4.44	gleysol		

Table 2 Temperature (°C), relative humidity (%) and CO<sub>2</sub> fluxes (mmol m<sup>-2</sup> d<sup>-1</sup>) from the soils of the drawdown area of the Nam Theun 2 Reservoir (Lao PDR).

Site	2010			2011			2013		
	Hum	Temp	CO <sub>2</sub> flux	Hum	Temp	CO <sub>2</sub> flux	Hum	Temp	CO <sub>2</sub> flux
MNR upland	17.5	25.7	265±37	18.3	24.4	328±43			
MNR interm. up				26.9	27.5	669±56			
MNR interm. down	19.6	32.3	201±19	23.7	29	251±99			
MNR shoreline	37	31.9	40	46.4	27.3	67±7			
RES3S upland	22.3	26.8	231	23.6	25.6	366±14			
RES3S interm.	49.5	27.4	184±50	30.2	26.1	186±57			
RES3 Sshoreline	42.3	28.3	503±97	25.6	19.8	391±23			
RES2S upland	19.9	26.4	183±1	24.5	25.2	531±41			
RES2S interm.	34.6	29.2	138±21	30.2	26.1	339±52			
RES2S shoreline	49.4	28.5	332±5	48.7	27.1	166±23			
RES8S upland	27.7	28.2	86±0	26.9	27.0	468			
RES8S interm. up	32.3	28.3	75±15	33.2	26.9	300±19			
RES8S interm. down	32.9	29.1	110±10	32.3	27.8	239±44			
RES8S shoreline	45.3	29.7	286±59	44.5	28.5	660±121			
RES8S' upland	32.6	32.5	342±70						
RES8S' interm.	35.9	31.9	143±24						
RES8S'shoreline	42.7	31.9	34±7						
RES4S upland	26.7	28.6	326±20	21.7	29.5	526±35	18.1	31.1	232±50
RES4S interm. up							24.3	28.7	196±29
RES4S interm. down	26.0	34.2	168±28	21.8	32.7	619±39	35.1	29.8	443±67
RES4S shoreline	44.6	31.1	34±7	18.3	32.1	115	51.2	29.6	393±57



Table 3: CO<sub>2</sub> emissions (in GgCO<sub>2</sub>.year<sup>-1</sup>) from the Nam Theun 2 Reservoir (Lao PDR) for the first five years after impoundment (2009, 2010, 2011, 2012 and 2013). Percentages between brackets represent the proportion of each component to the total annual emission.

Year	Ebullition	Diffusion (Reservoir)	Diffusion (Drawdown)	Degassing	Diffusion (Downstream)	Total
<b>2009</b>	1.2±0.5 (<1%)	730.0±46.2 (92%)	6.3±0.5 (1%)	52.7±14.9 (7%)	4.0±0.3 (<1%)	<b>794.1±48.5</b>
<b>2010</b>	1.04±0.5 (<1%)	538.57±28.6 (51%)	413.7±15.9 (39%)	85.37±17.4 (8%)	14.34±0.4 (1%)	<b>1053.0±37.0</b>
<b>2011</b>	1.06±0.5 (<1%)	345.88±24.3 (42%)	386.4±16.0 (47%)	84.03±10.7 (10%)	11.60±0.5 (1%)	<b>828.9±31.0</b>
<b>2012</b>	0.95±0.4 (<1%)	173.30±11.5 (23%)	572.3±19.9 (75%)	17.03±3.8 (2%)	2.23±0.2 (<1%)	<b>765.8±23.3</b>
<b>2013</b>	1.04±0.5 (<1%)	118.70±27.3 (21%)	419±15.0 (76%)	13.61±4.0 (2%)	1.43±0.2 (<1%)	<b>553.8±31.4</b>

Figure 1 Map of the Nam Theun 2 monitoring network. The station names are defined by numbers and an abbreviated name as follow: RES standing for reservoir, NTH for Nam Theun River, NON for Nam On River, NXT for Nam Xot, NPH1 for Nam Phao River, TRC for Tail Race Channel, REG for Regulatin Pond, DCH for downstream channel, NKT for Nam Katang River, NGM for Nam Gnom and XBF for Xe Bangfai River.

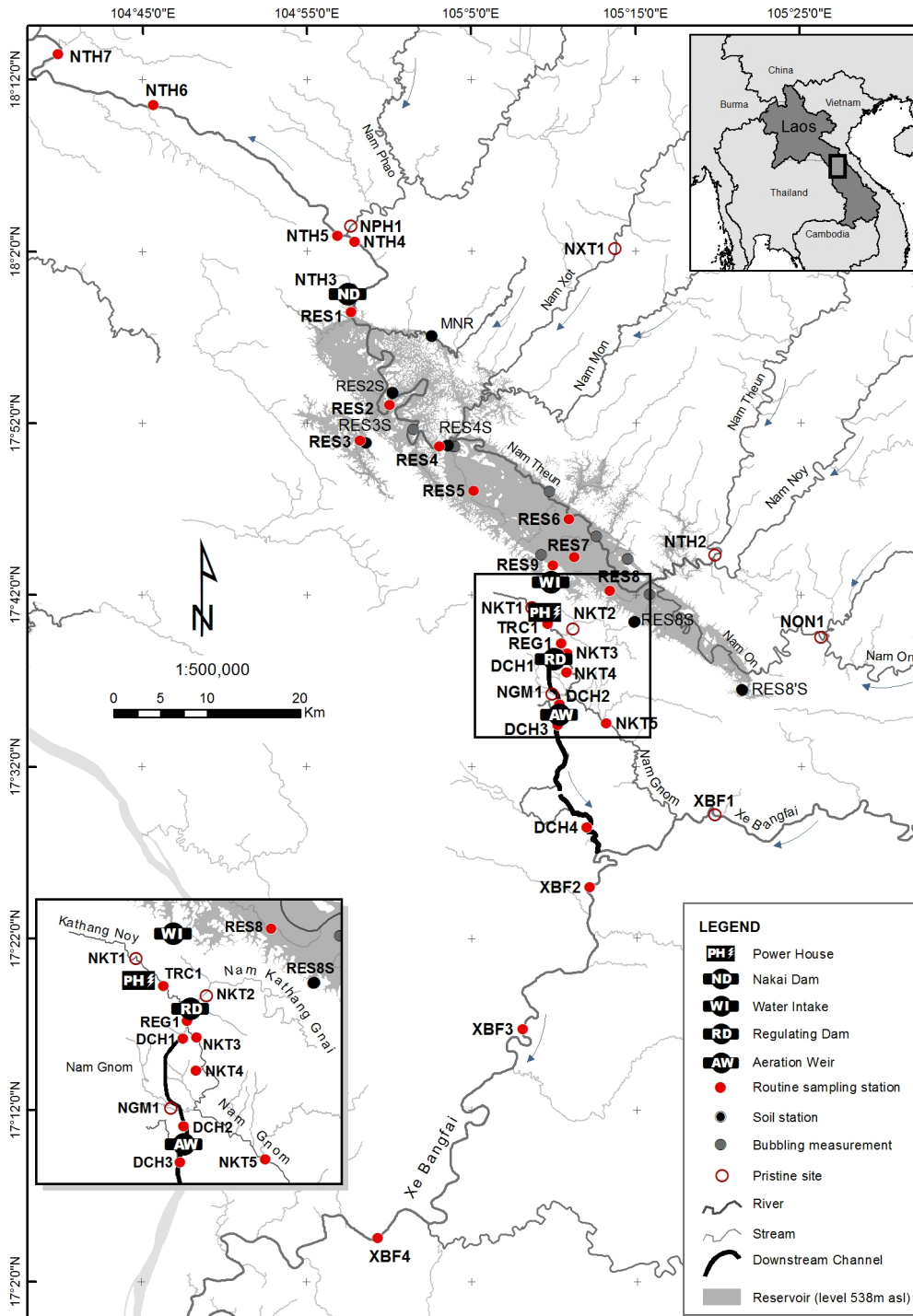


Figure 2 : Median and interquartile range (boxes), average (+), and full range of values (whiskers) of particulate organic carbon (POC), dissolved organic carbon (DOC), total inorganic carbon (TIC) and CO<sub>2</sub> concentrations in four pristine river of the Nam Theun watershed during three distinct seasons : cold dry (CD), warm dry (WD) and warm wet (WW) seasons. The dataset includes data from 2009 to 2013.

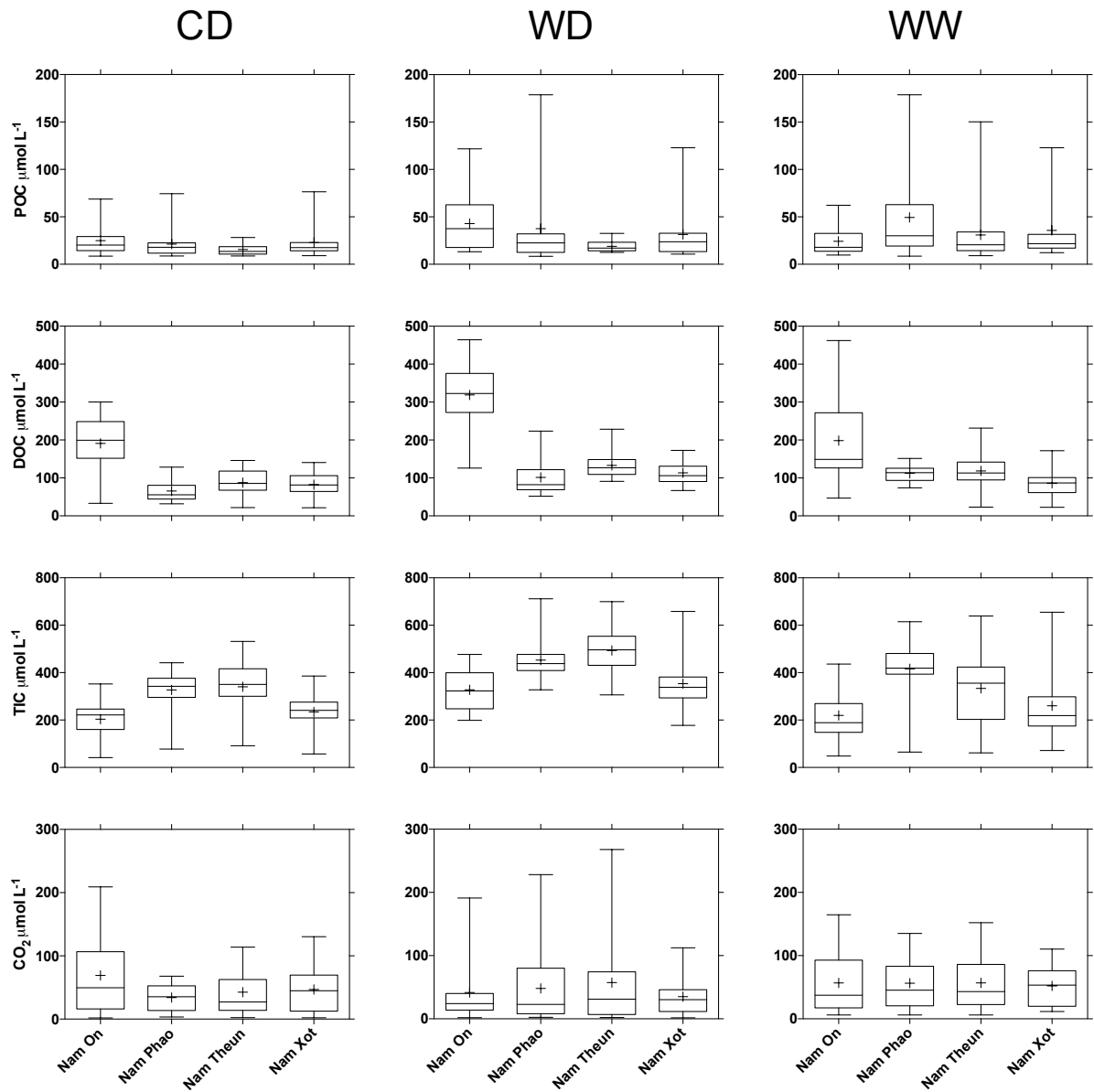


Figure 3: Total carbon inputs in form of particulate organic carbon (POC), dissolved organic carbon (DOC) and total inorganic carbon (TIC) from the Nam Theun watershed to the Nam Theun 2 Reservoir for four distinct years after reservoir impoundment.

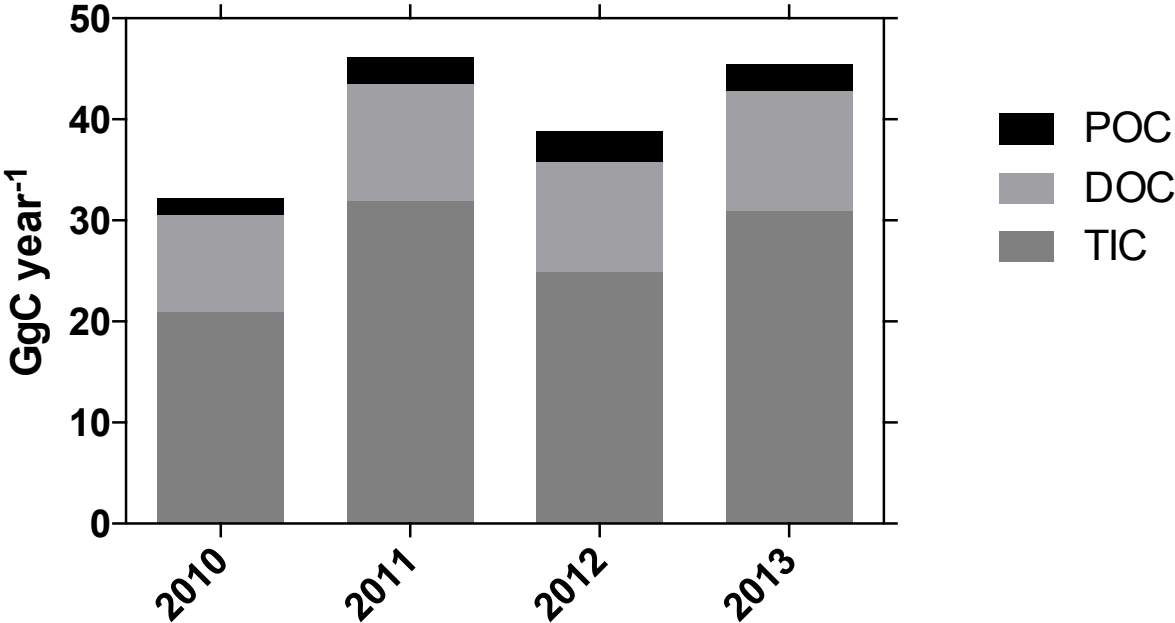


Figure 4: Temperature (grey solid circle) and oxygen (black solid circle), DOC (open square), POC (solid square) and CO<sub>2</sub>(triangle) concentrations in the Nam Theun 2 Reservoir water column during the cool dry, warm dry and warm wet seasons in 2011 at three stations (RES3, RES7 and RES9).

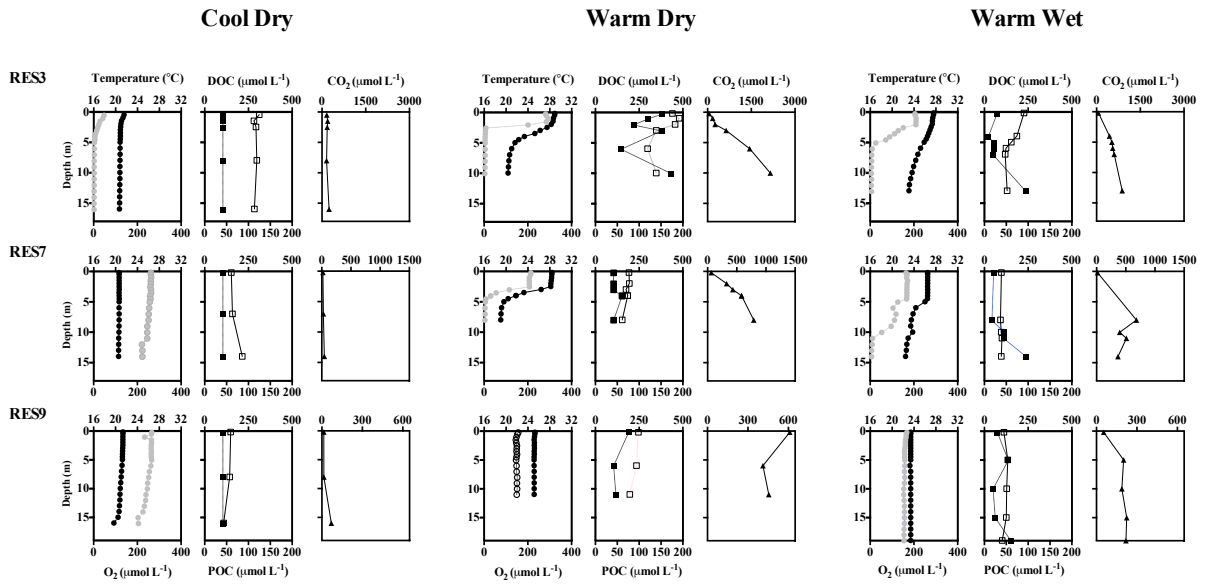


Figure 5: Monthly average CO<sub>2</sub> concentrations at the stations RES1-8 (a) and at the station RES9 (b), average diffusive fluxes at the stations RES1-8 (c) and at the station RES9 (d) and total monthly (e) and yearly (f) CO<sub>2</sub> emissions by diffusive fluxes from the Nam Theun 2 Reservoir (Lao PDR)

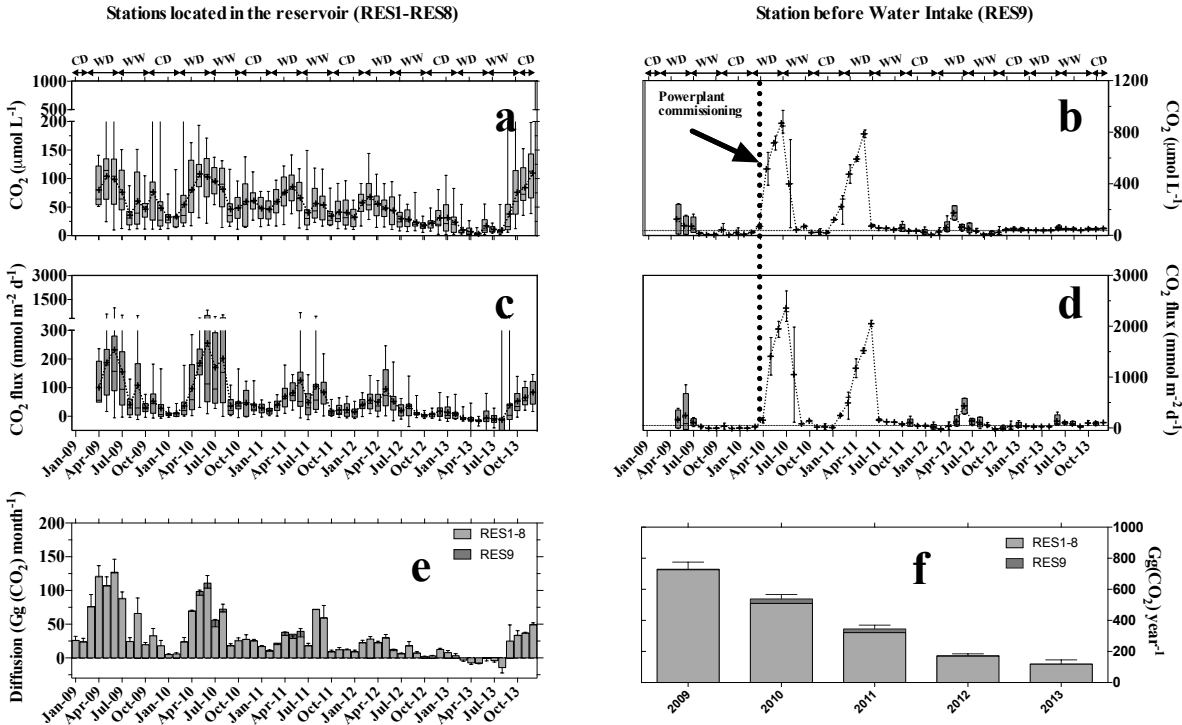


Figure 6: Diffusive fluxes and degassing below the powerhouse and the Nakai Dam on a monthly (a) and yearly basis (b) at the Nam Theun 2 Reservoir (Lao PDR). Note that degassing below ND includes spillway release (main contributor to 2009 and 2011 emissions below ND). Degassing below the powerhouse includes degassing immediately downstream of the turbines, downstream of the regulation dam and downstream of the aeration.

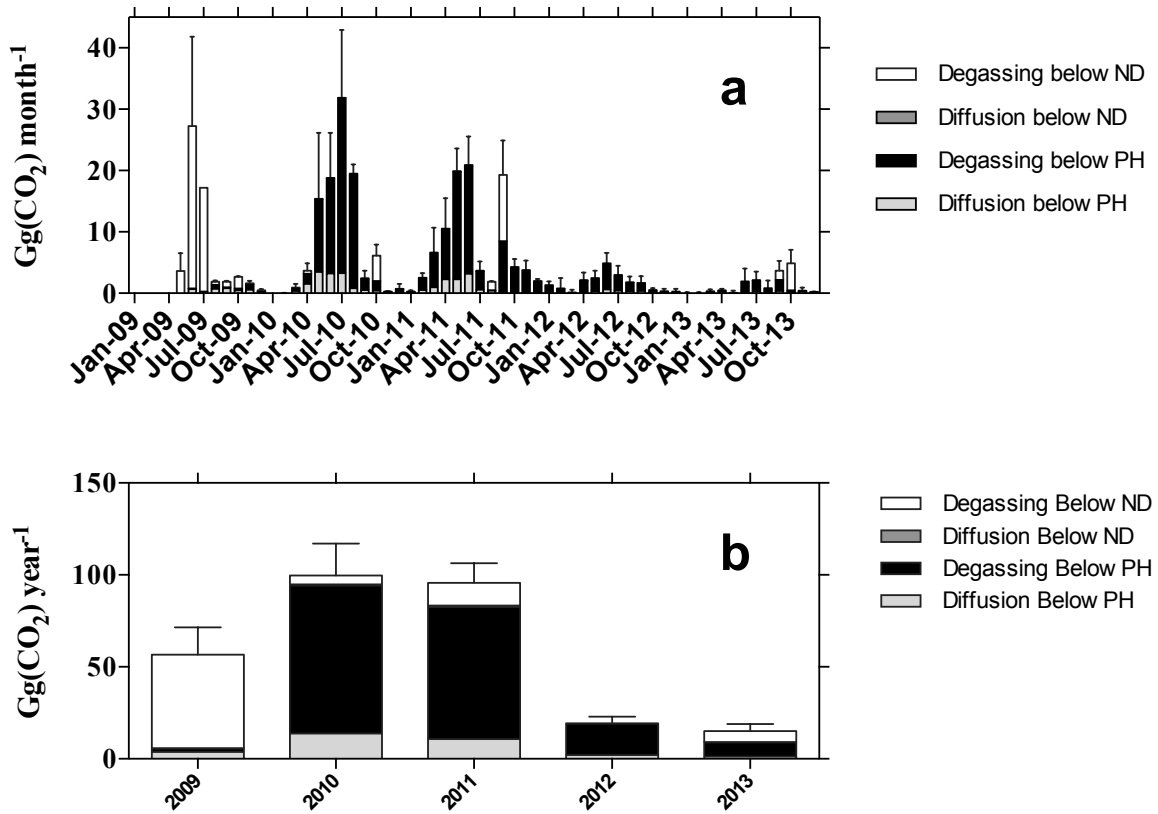


Figure 7: Monthly emissions from the drawdown area and variation of the area of the drawdown area of the Nam Theun 2 Reservoir (Lao PDR)

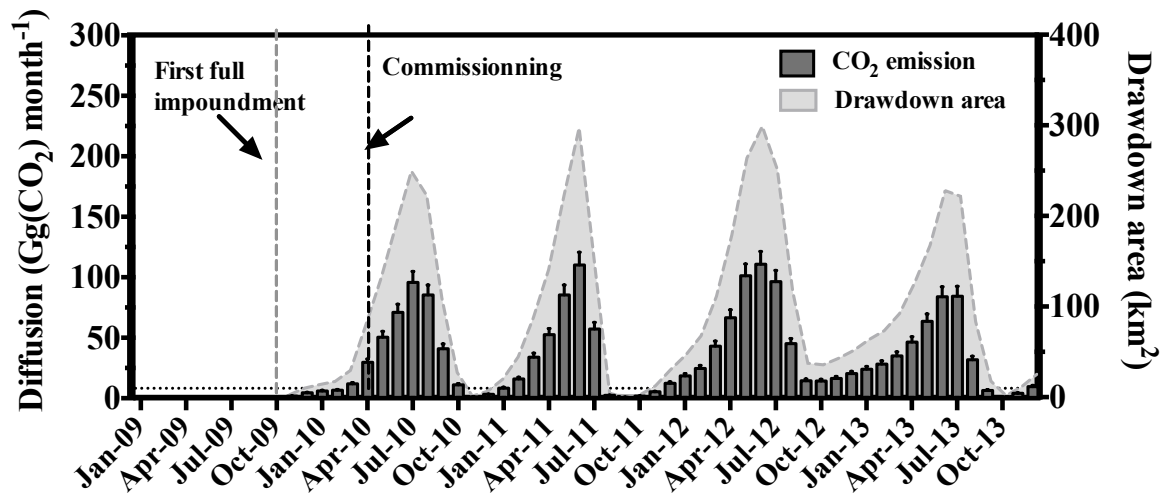




Figure 8: Monthly (a) and yearly (b) average of the total emissions from the Nam Theun 2 Reservoir by diffusion at the reservoir surface, diffusion from the drawdown area, ebullition, degassing and diffusion from the Nam Theun River and artificial channel at the Nam Theun 2 Reservoir (Lao PDR). On panel a, water level variations in the reservoir are given.

